2009

THE SECOND GENERATION PROTEASOME INHIBITOR CARFILZOMIB INTERACTS SYNERGISTICALLY WITH HDAC INHIBITORS IN DIFFUSE LARGE B-CELL LYMPHOMA CELLS THROUGH MULTIPLE MECHANISMS AND CIRCUMVENTS BORTEZOMIB RESISTANCE

Dmitry Lembersky
Virginia Commonwealth University

THE SECOND GENERATION PROTEASOME INHIBITOR CARFILZOMIB INTERACTS SYNERGISTICALLY WITH HDAC INHIBITORS IN DIFFUSE LARGE B-CELL LYMPHOMA CELLS THROUGH MULTIPLE MECHANISMS AND CIRCUMVENTS BORTEZOMIB RESISTANCE

A thesis submitted in partial fulfillment of the requirements for the degree of Master of Science at Virginia Commonwealth University.

by

DMITRY LEMBERSKY
Bachelor of Science, Christopher Newport University, 2007

Director:
Dr. Steven Grant, MD
Department of Biochemistry

Virginia Commonwealth University
Richmond, VA
May, 2009

ACKNOWLEDGEMENTS

I would like to thank the many different people who made this project possible:

My advisor, Dr. Steven Grant for giving me the direct opportunity to carry out this project

My committee members, Dr. Paul Dent and Dr. Daniel Conrad for their advice and support

Dr. Girija Dasmahapatra, for his guidance, training, patience, and support. I could not have done this project without his help

My friend and co-worker Leena Youssefian for her continual support and encouragement

Everyone in Grant Lab for their guidance and support

My family for their support and for standing by me during this time

TABLE OF CONTENTS

LIST OF FIGURES

LIST OF ABBREVIATIONS

7AAD - 7-amino-actinomycin D

ABC – Activated B-cell

GC – Germinal center

DLBCL – Diffuse large B-cell lymphoma

ER – Endoplasmic reticulum

HDAC – Histone deacetylase

HDACI – Histone deacetylase inhibitor

HL – Hodgkin's Lymohoma

NF-κB – Nuclear factor kappa B

NHL – Non-Hodgkin's Lymphoma

ROS – Reactive oxygen species

SAHA - suberoylanilide hydroxamic acid (vorinostat)

ShRNA **–** Short hairpin ribonucleic acid

ABSTRACT

THE SECOND GENERATION PROTEASOME INHIBITOR CARFILZOMIB INTERACTS SYNERGISTICALLY WITH HDAC INHIBITORS IN DIFFUSE LARGE B-CELL LYMPHOMA CELLS THROUGH MULTIPLE MECHANISMS AND CIRCUMVENTS BORTEZOMIB RESISTANCE

By Dmitry Lembersky, Bachelor of Science

A thesis submitted in partial fulfillment of the requirements for the degree of Master of Science at Virginia Commonwealth University.

Virginia Commonwealth University, 2009

Major Director: Dr. Steven Grant, MD
Department of Biochemistry

Mechanisms underlying the interactions between the proteasome inhibitor carfilzomib and HDAC inhibitors were examined in both germinal center (GC) and activated B-cell (ABC) subtypes of human diffuse large B-cell lymphoma (DLBCL). Simultaneous exposure to minimally toxic concentrations of carfilzomib and HDAC inhibitor vorinostat resulted in the release of mitochondrial pro-apoptotic proteins SMAC and cytochrome c, pro-apoptotic caspase activation, and synergistic induction in apoptosis in both ABC and GC DLBCL subtypes. These events were associated with a marked increase in the stress kinase JNK, ROS generation, G2-M cell cycle arrest, as well as induction of DNA damage. Genetic knockdown of JNK resulted in a significant decrease in carfilzomib/vorinostat induced cell death. Co-administration of the antioxidant MnTBAP significantly reduced carfilzomib/vorinostat induced cell death, and resulted in a marked decrease in caspase-3 as well as a striking decrease in JNK phosphorylation. Tumor

growth reduction was also observed in animal models that were treated with a combined regimen of carfilzomib and vorinostat. Finally, the combined treatment of carfilzomib/vorinostat was able to overcome any cross-resistance to carfIlzomib in bortezomib resistant cells. Collectively, these finding indicate that the combined regimen of carfilzomib and HDAC inhibitors promote lethality in ABC and GC human DLBCL cells by a variety of mechanisms both *in vitro* and *in vivo*. Further studies are necessary for clinical development of this drug regimen.

INTRODUCTION

LYMPHOMA

The groups of cancers under the general term lymphoma are very broad, and symbolize the disease of the impaired immune system. This includes lymphomas of B-cell origin, T-cell origin, and natural killer cell origin. Lymphomas are broadly classified into two major groups i.e. Hodgkins (HL) and Non-Hodgkin lymphoma (NHL). The classifications are based on the differences in characteristics, morphology of the cancerous cells and prognosis with current therapy.

Diffuse lymphocytic B-cell lymphoma (DLBCL) is the most frequently encountered lymphoma in adults, accounting for 30-40% of adult neoplasms (1). It is an aggressive malignancy of mature B lymphocytes, with 25,000 new cases annually, accounting for roughly 40% of cases of non-Hodgkin's lymphoma. Patients with DLBCL have highly variable clinical outcomes; although most patients respond initially to chemotherapy, fewer than half of the patients achieve a durable remission (2). Although treatment progress, including the development of chemotherapeutic regimens such as R-CHOP or advances in bone marrow transplantation have led to an improved prognosis (3), many patients become resistant to standard therapy and succumb to their disease. Consequently, novel treatment approaches continue to be sought.

Recently, microarray analyses performed on untreated DLBCL has lead to the identification of two main sub-types, germinal center (GC-DLBCL), and activated B-cell (ABC-DLBCL). Both have a distinct gene expression profile, characteristic of either

normal germinal center b-cells or activated blood memory b-cells (4). The germinal center-like subgroup is correlated with a significantly better prognosis in comparison with the activated b-cell like subgroup (4), and the 5-year survival rate of both is 59% and 30% respectively (5). A third subgroup is comprised of cases that do not express the genetic profile of wither the ABC or GC subgroups, yet has a poor prognosis similar to that of the ABC subgroup (4). Different oncogenic mechanisms underlie both the ABC and GC subgroups, with Bcl2 gene rearrangement occurring almost exclusively with the GC subgroup (4,6-8), while NF-κB signaling activation occurs in the ABC subgroup (4). Such findings raise the possibility that novel therapies may ultimately be targeted to specific DLBCL sub-types (5,6).

The PROTEASOME

The two main routes of protein degradation are proteasomes and lysosomes. While lysosomes degrade extracellular and transmembrane proteins, proteasomes primarily degrade intracellular proteins. This could be due to phosphorylation by signaling pathways, or they could be recognized as being misfolded. The proteins are tagged for degradation via an ubiquitin tag (9).

The functionally active 26S proteasomes is an ATP-dependent proteolytic complex, located in the cytoplasm and nucleus of eukaryotic cells. It is made up of a 20S core catalytic subunit, capped by both ends by 19S regulatory subunits (9,10). Generally, the proteasome identifies proteins destined for degradation by their ubiquitin tag, although ubiquitination is not always necessary for degradation of every protein (9).

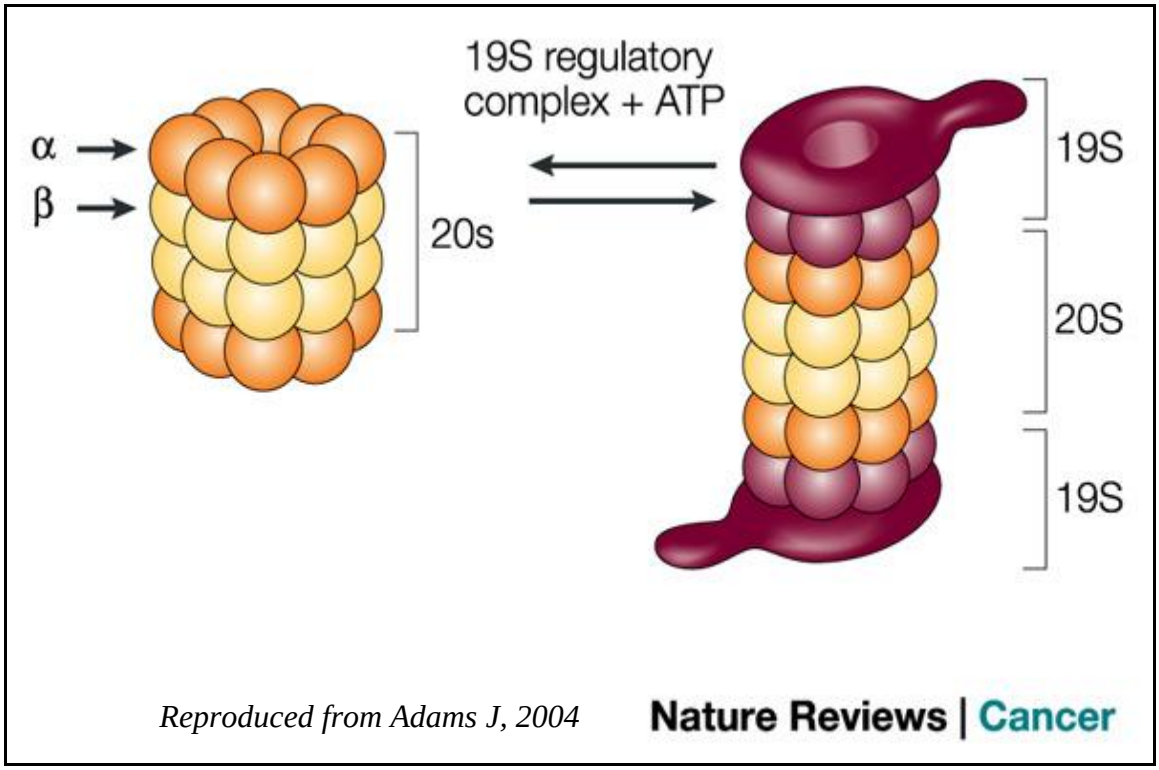

Reproduced from Adams J, 2004

The 20S proteasome subunit is a cylindrical structure composed of 28 protein subunits, organized into 4 stacked rings. The top and bottom rings are formed by 7 polypeptides, termed α-subunits, and the two inner rings are made up of 7 β-subunits. The β-subunits contain the enzymatically active sites of the proteasome (9). The β1, β2, and β5 subunits are characterized as chymotryptic-like, tryptic-like, and post-glutamyl peptidyl hydrolytic-like (9,11-13).

The 19S regulatory complex contains 20 subunits which bind to both ends of the 20S proteasomes to form the 26S proteasomes (9). ATP hydrolysis is required for both the formation of the 26S complex and for unfolding proteins for entry into the catalytic core of the proteasomes (9,12,14). It is therefore possible that the increasing protein

degradation requirements in rapidly proliferating cancer cells make them more susceptible to proteasomal inhibition (15).

Targeting the majority of proteins to the proteasome for degradation requires polyubiquitination, but it can also serve as a signal for trafficking, kinase activation, and other nonproteolytic activities (9,16). Conjugation of ubiquitin to a target protein proceeds in via a three-step mechanism. Initially, ubiquitin is activated in its C-terminal glycine by the ubiquitin-activating enzyme, E1. Following activation, one of several E2 enzymes (ubiquitin-conjugating enzymes) transfers ubiquitin from E1 to a member of the ubiquitin-protein ligase family, E3, to which the substrate protein is specifically bound. This enzyme catalyzes the last step in the conjugation process, covalent attachment of ubiquitin to the substrate (11). Ubiquitination is not absolutely required for proteasomal degradation however, as the tumor suppressor RB family proteins can undergo proteasomal degradation through a ubiquitin-independent pathway.

ER STRESS AND THE UNFOLDED PROTEIN RESPONSE

An excessive accumulation of misfolded proteins within the ER-Golgi network elicits a cellular response which initially promotes cell survival, but will lead to apoptosis if the repair mechanisms are overwhelmed (15). The core of this defense system is known as the unfolded protein response (15,17), which functions to increase expression of protein chaperones such as Grp78/BiP, in order to limit protein aggregation, to increase biosynthesis of structural components of the ER, and to inhibit overall protein synthesis so that the load on the ER-Golgi network is reduced. Upstream control of the

unfolded protein response is mediated via activation of three ER transmembrane proteins, the serine/threonine kinase PERK, IREα and the bZIP transcription factor, ATF6 (15,17,18).

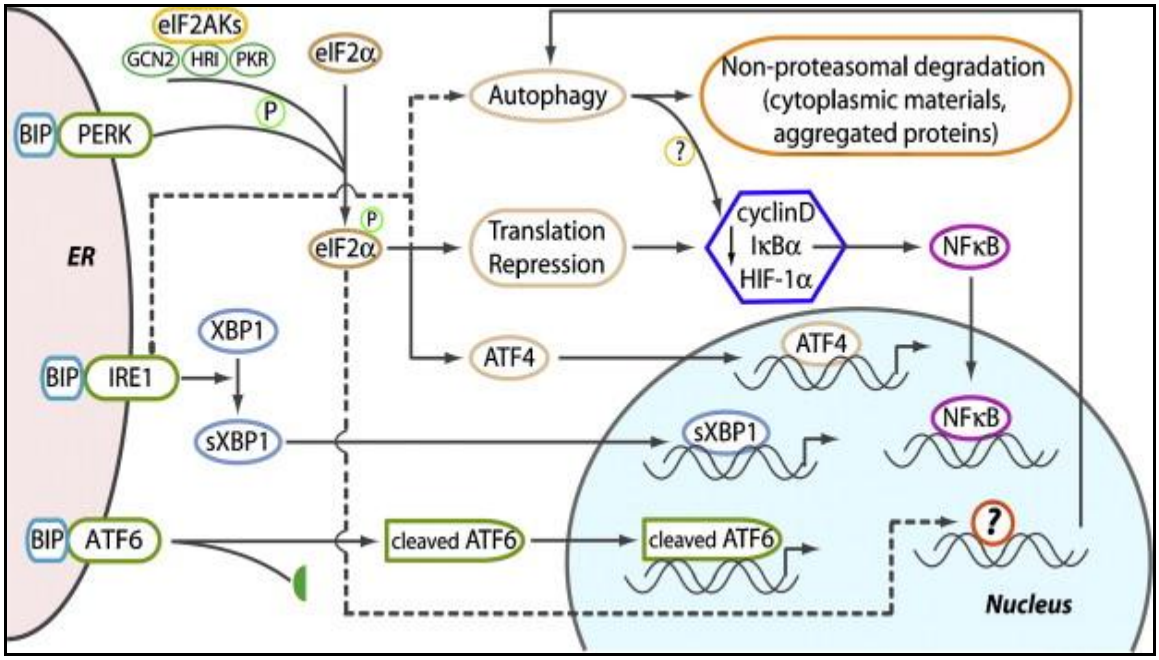

The unfolded protein response (UPR). In response to a build-up of misfolded proteins within the endoplasmic reticulum (ER), the molecular chaperone glucose regulated protein-78 kD (Grp78, commonly known as BiP) dissociates from the luminal domains of PKR-like ER kinase (PERK), IRE1, and ATF6, resulting in their activation. PERK-mediated phosphorylation of eIF2α coordinates activation of the transcription factor ATF4 with attenuation of global protein synthesis and activation of autophagy. Reproduced from McConkey DJ, et al, 2008.

It is unknown exactly how proteins are shuttled to the proteasome for degradation, but current evidence points to discrete structures known as aggresomes (15,19-21), as well as the cytosolic chaparone, HSP70 (15,22). The activity of proteasome inhibitors may be improved by blocking proteasome inhibitor-induced aggresome formation with pan-

specific chemical HDAC inhibitors such as trichostatin A or vorinostat (SAHA) (15,23,24). It has been shown that chemical pan HDAC inhibitors are some of the most potent PI-sensitizing agents, capable of restoring PI sensitivity in cells that are completely resistant to the agents basally (15,24).

EFFECT OF PROTEASOME FUNCTIONS ON SIGNALLING

It is known that many proteasome substrates are mediators of pathways which are disregulated in cancers (9), in addition to it's conventional role of inhibition of proteasome synthesis. It is reported that proteasome inhibitors modulate targets which govern the growth and survival of transformed cells like cell cycle, NF-κB, aggresome formation, stress pathways like SAPK/JNK etc. The proteasomes affects cell-cycle progression by regulating cyclins, and can also increase or decrease apoptotic activity via caspases, Bcl-2, and NF-κB (9). Proteasome inhibition can destabilize the regulation of CDC25A, CDC25C, KIP1 and the cyclins, which

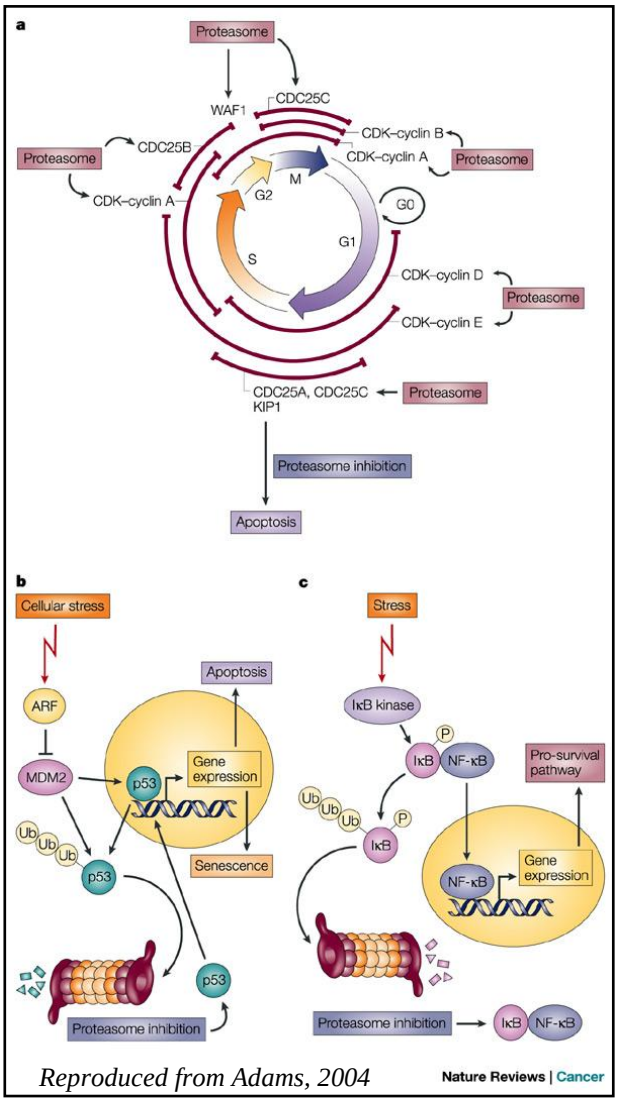

Reproduced from Adams, 2004

will make the cell more susceptible to apoptosis. Because of the fact that cell cycle checkpoints in cancer cells are disrupted, the cells may be more heavily dependent on proteasome-mediated degradation of cell cycle regulators, both positive regulators like cyclins and negative regulators like p21 and p27, for their survival (15).

The NF-κB family of transcription factors represents proteins bound to the inhibitor IκB, which while bound, remain inactive in the cytoplasm. In response to cellular stress, the IκB inhibitor becomes deactivated by the proteasome, which results in NF-κB translocation into the nucleus and activates several pro-survival pathways (9). NF-κB has been shown to control cell proliferation by activating genes such as interleukin 2 (IL-2) and CD40 ligand, all of which are factors that promote proliferation of lymphoid and myeloid cells (25). In addition, NF-κB has been shown to inhibit programmed cell death (25-29) by activation of genes known to block apoptosis via TNFα, as well as others (25,30). The genes that are induced by NF-κB include cellular inhibitors of apoptosis, caspase-8/FADD, and members of the Bcl-2 family of proteins (25,30).

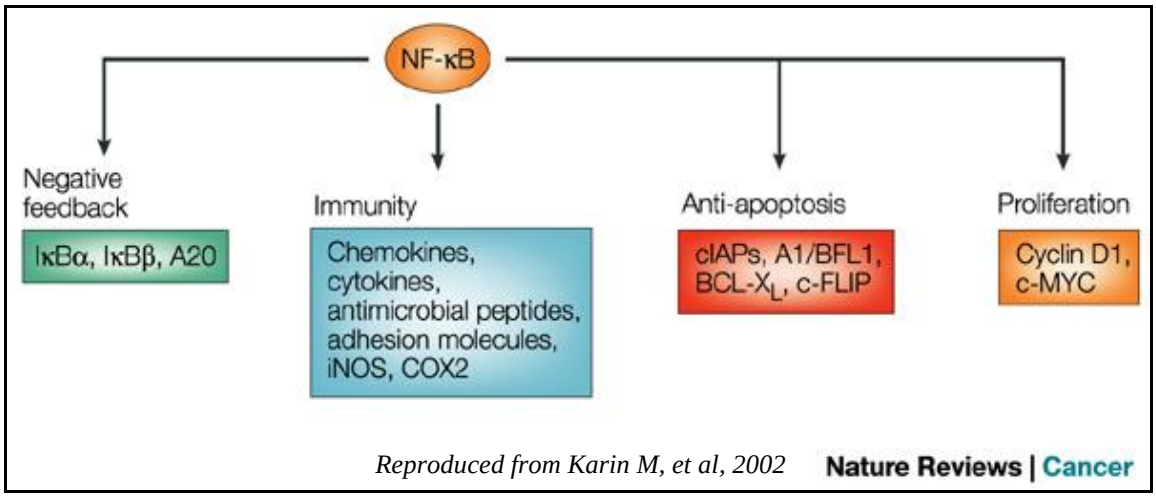

NF-κB has also been shown to attenuate apoptotic responses to genotoxic anticancer drugs and ionizing radiation (25,29-31), and that inhibition of NF-κB pushes chemoresistant tumors toward apoptosis (31). In addition to conferring resistance to cancer therapies, the anti-apoptotic activity of NF-κB can also have an important role in the emergence of neoplasms, by preventing the death of cells that have undergone chromosomal rearrangements or other types of DNA damage (25). Diffuse large B-cell lymphomas that are of the activated B-cell (ABC) phenotype have elevated expression of NF-κB target genes, which encode cytokines, chemokines and anti-apoptotic proteins (25), and expression of a non-phosphorylateable IκB mutant (super-repressor) in these cells inhibits their proliferation (25). In contrast, DLBCLs with a germinal-centre-like gene-expression profile seem to be resistant to the IκB super-repressor, which indicates that the canonical NF-κB signaling pathway, which depends on the IKKβ catalytic subunit and IκB degradation, is constitutively active in the activated B-cell-like DLBCL cells (25).

Reactive oxygen species (ROS) generation can result in DNA damage as well as oxidation of fatty acids and proteins. Eukaryotic cells continually produce ROS by electron transfer reactions, but ROS can be exacerbated by exogenous sources such as UV light, toxins, or drugs (32). NF-kB is considered a primary oxidative stress-responsive transcription factor that enhances the transcription of a variety of genes, including those for cytokines and growth factors, adhesion molecules, immunoreceptors, and acute response proteins (32). Most if not all agents that activate NF-κB also trigger ROS formation

It is well known that apoptosis requires a cascade of biochemical events, performed via a family of cysteine proteases called caspases (9). Caspase-9 is the apical caspase, which directly activates caspases -3 and -7 through proteolytic cleavage (33). Active caspase-3 processes caspases -2 and -6, and activated caspase-6 activates caspases -8 and -10 (33). Specifically, it is thought that caspase-8 and caspase-3 are the major effector caspases, essential for the apoptosis cascade (9,34). Activation of caspase-2 is caused by cytotoxic stress, and is required for permeabilization of the mitochondria and the release of SMAC and cytochrome c (35). Cytochrome c binds to Apaf-1 and activates caspase-9, which in turn, activates caspase-3 (35). Caspase-4 on the ER is thought to play a role in ER stress-induced apoptosis (36). Caspase precursors are constitutively expressed in the cell, and have to be activated via proteolytic cleavage by specific inducers. Activation of NFκB can inactivate caspase-8 (9,37), therefore proteasome inhibition could prevent activation of the anti-apoptotic factor NF-κB, potentiate caspase activity, and induce apoptosis.

PROTEASOME INHIBITORS

Proteasome inhibitors might be natural or synthetic and five important classes of proteasome inhibitors exist: peptide aldehydes, peptide vinyl sulphones, peptide boronates, peptide epoxiketones and β-lactones (9). The natural inhibitor lactacystin and synthetic peptide aldehydes were the first agents to be identified with the ability to inhibit proteasomes, yet they suffered from several limatations including poor stability and bioavailability, and lack of specificity (9,38). Substituting the aldehyde with boronic acid

would enable the compound to achieve a covalent, reversible interaction with proteasomes, while achieving improved potency and selectivity. (9,38,39). Bortezomib was one of the original 13 boronic-acid proteasome inhibitors selected for further study (9). Studies have shown that the proteasome inhibitor bortezomib induced ROS formation, and played a critical role in caspase-9 activation in bortezomib-mediated apoptosis (40).

BORTEZOMIB

Bortezomib was originally synthesized in 1995 as MG-341 .It was developed by Millennium Pharmaceuticals. After promising preclinical results, the drug (PS-341) was tested in a small Phase I clinical trial on patients with multiple myeloma (MM) cancer. When one of the first volunteers to receive the drug in the clinical trial achieved a complete response, the drug was given priority at the company, and in 2003, bortezomib (Velcade) was approved for use in multiple myeloma by the FDA based on the results of the SUMMIT Phase II trial (38).

Bortezomib is known to bind with 26S proteasome reversibly and cleared very rapidly from the plasma compartment; achieving 90% clearance within 15 minutes of intravenous administration (38). There is minimal intersubject and intrasubject variation in proteasome activity. The effects of bortezomib are dose related, achieving 80% proteasome inhibition at a dose of approximately 1.96 mg/m^2. Monitoring the extent of 20S proteasome inhibition in PBMCs collected from patients enrolled in Phase I clinical trials confirmed that levels of inhibition up to 80% did not cause excessive toxicity

(15,38,41-43). Bioassay testing in rats indicated that most organs received a similar amount of drug, with no drug present in the testes, eyes, and central nervous system (38). Proteasome activity is restored 48 to 72 hours after cessation of bortezomib treatment (38).

CARFILZOMIB (PR171)

Carfilzomib is an epoxyketone that was developed by Proteolix, Inc. (South San Francisco, CA, USA) (15,44). Carfilzomib differs from bortezomib in that it is a irreversible proteasome inhibitor, and it is more selective for the chymotryptic activity (15,44). More importantly however is the fact that it can be given at a much more aggressive schedule, ie: doses that cause greater than 80% proteasome inhibition for at least 5 consecutive days (15,44). Preclinical studies also indicate that PR171 is active against solid tumors as well as cell lines from patients resistant to bortezomib (Proteolix pipeline). Recent published result has indicated that carfilzomib is active against bortezomib resistant cells (45).

HISTONE PROTEINS

Transcription in eukaryotic cells depends on the manner in which the DNA is packaged (46,47). DNA is tightly compacted into the highly organized protein-DNA complex chromatin in resting cells to prevent access by transcription factors, thereby preventing replication. The fundamental subunit of chromatin is called the nucleosome,

which is composed of an octamer of 4 core histones, for example a H3/H4 tetramer and two H2A/H2B dimers, surrounded by 146 bp of DNA, Fig. (46). During activation of transcription, this compact, inaccessible DNA is made available to replication proteins via nucleosome modification. (46,48).

HISTONE DEACETYLASES

Histone tails are positively charged, due to the amine groups present on their lysine and arginine amino acids. This allows the positively charged histone tails to interact with the negatively charged phosphate groups on the DNA backbone, keeping the DNA tightly compacted. Acetylation partially neutralizes the positive charges of the histones, allowing for chromatin expansion and gene transcription (49). This process involves the transfer of an acetyl group from the acetyl coenzyme A metabolic intermediary to the ε-amino group of lysine residues in histone tails, catalyzed by a group of enzymes known as histone acetyltransferases (HAT) (49). Histone deacetylases remove these acetyl groups, thereby condensing the DNA and promoting transcriptional repression (49).

HISTONE DEACETYLASE INHIBITORS (HDACi)

Histone deacetylase inhibitors (HDACi) can elicit a range of responses that affect tumor growth and survival, including inhibition of cell cycle progression, induction of tumor cell-selective apoptosis, suppression of angiogenesis, and modulation of immune responses, as well as show promising activity against hematological malignancies in

clinical trials (50). A major mechanism of apoptosis induction by HDAC inhibitors is through the induction of oxidative injury, or ROS formation (51). HDAC inhibitors are considered to be among the most promising agents in drug development for cancer therapy (52-54), largely because it has been shown that these inhibitors present relatively low toxicity to normal cells, most likely due to the fact that normal cells are relatively resistant to HDACi-induced cell death, whereas a broad variety of transformed cells are sensitive to HDAC-induced cell death (52). There are both natural and synthetic HDAC inhibitors, and they can be divided into several groups: hydroxamic acid derivatives, cyclic peptides, short-chain aliphatic acids, and benzamides (52).

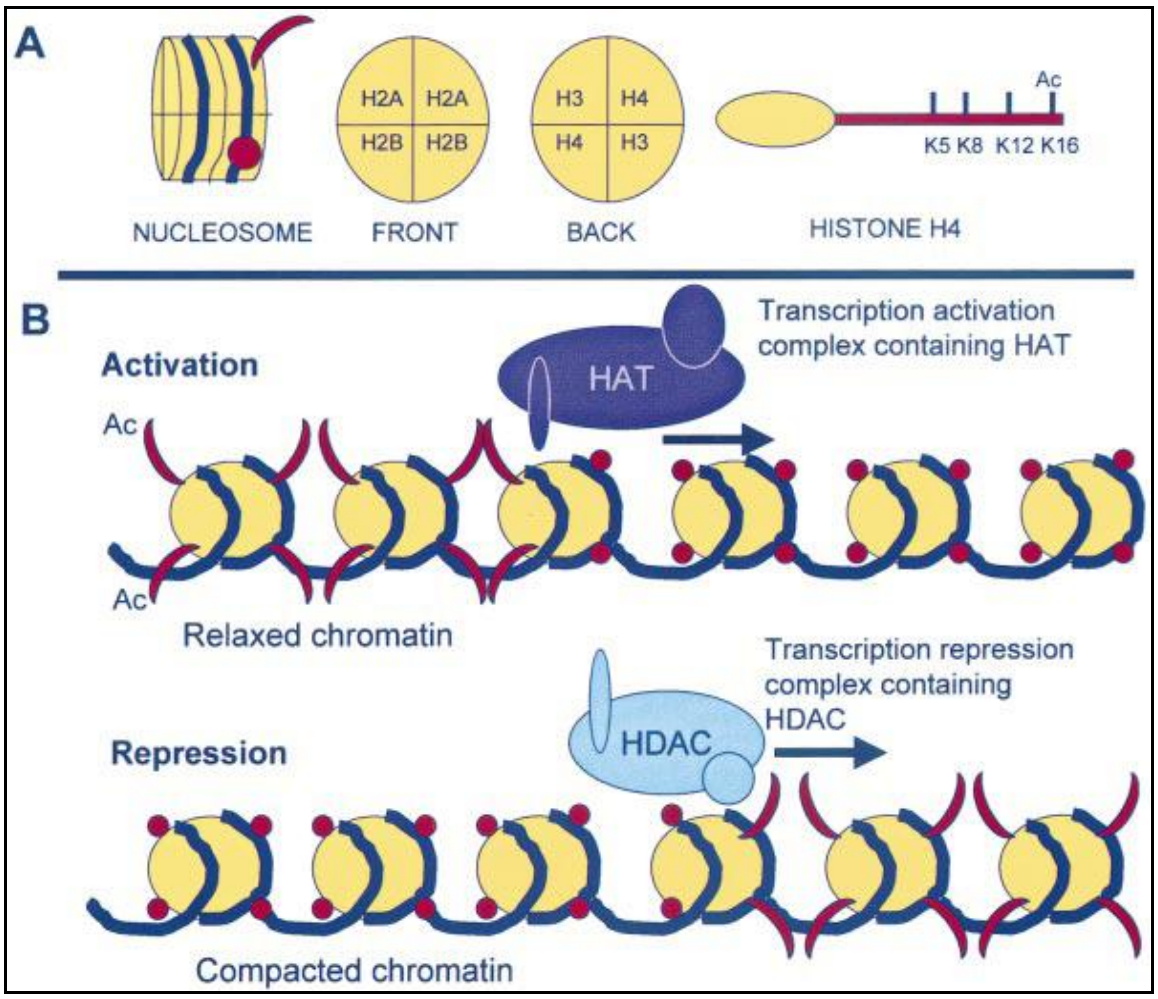

Schematic representation of a nucleosome. Yellow represents the histones. Dark red depicts the histone tail that can be modi®ed to loosen DNA (purple) winding. The dark red circle represents a tail without an acetyl (Ac) group. The dark red ` banana shape ' represents a histone tail with an acetyl group, relieving the tight packaging of the DNA. (B) Transcriptional repression and activation in chromatin. Yellow circles represent core histone octamers ; in the upper panel, acetylated histone tails (dark red) are depicted emerging from the octamer (46). Reproduced from de Ruijter, et al, 2003

VORINOSTAT (SAHA)

Vorinostat (SAHA, Zolinza) is a hydroxamic acid derived synthetic compound, and a pan-inhibitor of Class I and II HDACs (52,55). It is the first HDAC inhibitor

approved for clinical use in cancer patients for treating cutaneous T-cell lymphoma by the US Food and Drug Administration. It has been shown to induce cell cycle arrest and apoptosis and prolong survival in preclinical models of B-cell lymphoma (50,56), and Phase I trials are showing promising results (56-58). It is likely necessary to use vorinostat in combination with other drugs for enhanced therapeutic effects (52). Already, HDACi have been shown to cooperate with radiation therapy, antitubulin agents, topoisomerase I and II inhibitors, cisplatin, the kinase inhibitor imanitib, proteasome inhibitors such as bortezomide, the heat shock protein-90 inhibitor 17-N-allylamino-17-demethoxygeldanamycin, the Her2 receptor inhibitor trastuzumab, retinoids, inhibitors of DNA methylation, estrogen receptor antagonists, dexamethasone, and others (52).

RATIONALE FOR COMBINING CARFILZOMIB AND VORINOSTAT

Owing to the poor prognosis of DLBCL patients to bortezomib therapy, newer and more effective proteasome inhibitor was sought. Development of second generation proteasome inhibitor i.e. carfilzomib was a step in this direction. A combined drug regimen to potentiating the activity of carfilzomib will be an attractive option. There are multiple reasons suggesting combination of carfilzomib and vorinostat may result in a synergistic interaction. There is evidence that HDAC inhibitors activate the NF-κB survival pathways (59), whereas proteasome inhibitors block this activation (15). There is also evidence that proteasome inhibitors like bortezomib induce aggresome formation (60), which promotes cell survival, whereas HDAC inhibitors block the same (15,23,24).

In addition, both HDACI and proteasome inhibitors have been shown to induce ROS generation and oxidative stress (40,51). Therefore, combining the two may result in a synergistic interaction. Bortezomib and vorinostat have also been shown to interact synergistically in many cancer cell types, including hematologic malignancies as well as solid tumors and under clinical trials. In light of all this evidence we propose that combining carfilzomib and vorinostat will result in a synergistic interaction with respect to cell death in both GC and ABC DLBCL cell lines.

MATERIALS AND METHODS

Cells

SUDHL16 cells (GC subtype) was a kind gift from Dr. Alan Epstein, University of Southern California, LA. SUDHL4, SUDHL6 (both GC), OCI-LY10, OCI-LY3 (both ABC) were provided by Dr. Lisa Rimsza of University of Arizona, Tucson. Bortezomib-resistant SUDHL16-10BR (GC) and SUDHL6-20BR (GC) were generated by exposing the respective parental cells to progressively increasing concentrations of bortezomib beginning with 1.0 nM. Once cells developed resistance to bortezomib, they were cultured in the absence of drug for two weeks prior to experiments. Multiple studies documented the persistence of drug resistance under these conditions. SUDHL-10BR (GC) and Raji-20BR were generated by exposing the respective parental cells to progressively increasing concentrations of bortezomib beginning with 1.0 nM. Once cells developed resistance to bortezomib, they were cultured in the absence of drug for two weeks prior to experiments. Multiple studies documented the persistence of drug resistance under these conditions. SUDHL16-sh-JNK cells were generated by electroporation (Amaxa, GmbH, Germany) using buffer L of a MAP8 shRNA (SuperArray Bioscience Corporation, Frederick, MD) into SUDHL16 parental cells according to the manufacturer's instructions. Stable clones were selected by serial dilution using G418 as selection marker.

Cell Culture

Cells were suspended in sterile plastic T-flasks (Corning, NY) and placed in a 5% CO_2, 37^0C incubator. Cells were counted on a Coulter Counter Cell and Particle Counter, and split when their counts were at least 9.0 x 10^5 cells/mL, using RPMI media containing L-glutamine, pen-strep, non-essential amino acids, all provided by Invitrogen, and sodium pyruvate and RPMI provided by Mediatech, Manassas, VA. All experiments were carried out within passage 6-24 to ensure uniformity of drug responses.

Reagents

Carfilzomib (PR171 and PR-047) were provided by Proteolix, San Francisco, CA. Bortezomib (Velcade) was provided by Millennium Pharmaceuticals, Cambridge, MA. MnTBAP was provided by Calbiochem, CA. N-Acetyl-L-cysteine was provided by Sigma-Aldrich, St. Louis, MO. 5-(and-6)-chloromethyl-2',7'-dichlorodihydrofluorescein diacetate, acetyl ester (ROS dye) was provided by Molecular Probes, Eugene, OR. 7-Aminoactinomycin D was provided by Sigma-Aldrich, St. Louis, MO.

Experimental Format

Logarithmically growing cells were suspended in sterile plastic T-flasks (Corning, NY), or sterile plastic cell culture plates (Greiner), in media containing 10% FBS (Atlanta Biologicals, Lawrenceville, GA). Cells were cultured at least 24 hours prior to treatment with designated drugs. The flasks and plates were then placed in a 5% CO_2,

37^0C incubator for various intervals. At the end of the incubation period, cells were transferred to sterile centrifuge tubes, pelleted by centrifugation at 400 x g for 10 min at room temperature, and prepared for analysis as described below. All cells were tested regularly for mycoplasma contamination using the MycoAlert Mycoplasma Detection Kit, provided by Lonza, Inc., Rockland, ME, to insure that cells were free of mycolpasma prior to experimentation. All experiments were performed using equivalent cell concentrations (e.g.,4.0-5.0 x 10^5 cells/ml) to ensure conformity of drug responses.

Assessment of cell death

Drug effects on cell viability were monitored by flow cytometry using 7AAD as the staining dye. Briefly, cells were stained with 25 μM 7AAD solution at room temperature in regular culture media and analyzed in the FL2 channel using the Becton Dickinson flow cytometer. Alternatively, cells were washed with 1x PBS and stained with Annexin V/PI (BD PharMingen, San Diego, CA) for 30min. at room temperature. Cells were then processed and analyzed using the cytofluorometer. Cells undergoing apoptosis were also periodically monitored by Annexin V staining to confirm 7AAD results. Cells were also analyzed for viability using the VIACOUNT reagent in conjunction with a GUAVA PCA instrument using CytoSoft software as per the manufacturer's instructions. Results were verified by Trypan blue staining and enumeration of Trypan blue excluding cells using a hemocytometer. Results for each of these methods were found to be in good agreement.

Collection and processing of primary cells

Primary DLBCL cells obtained with informed consent from the bone marrow of a patient with DLBCL and extensive marrow infiltration (>70%). These studies have been approved by the Investigational Review Board of Virginia Commonwealth University. Bone marrow samples were collected in sterile syringes containing heparin and processed by standard techniques to separate mononuclear cells, after which $CD34^+$ cells were isolated using an immunomagnetic bead separation technique as we have previously described in detail (61). $CD34^+$ cells were then suspended in RPMI1640 medium containing 10% FCS and exposed to agents as described above for continuously cultured cell lines.

Western blot Analysis

Western blot samples were prepared from whole cell pellets. Equal amounts of protein (30μg) were separated by 4-12% Bis-Tris (Invitrogen) precast gel and probed with primary antibodies of interest as we have described in detail previously (61). The sources of primary antibodies were as follows: AIF, cytochrome c, p-JNK, JNK1, p-ERK, ERK, Mcl-1, Bak, Bid, Bcl-$x_{L,}$ CD20, Bax, Bak, IREα, GRP94, GRP78, XBP, p-c-Jun, c-Jun, NOXA, Bim and PUMA were from Santa Cruz Biotechnology, Santa Cruz, CA.; cleaved caspase-8, cleaved caspase-3, p-p38, p38 , p-eIF2a, eIF2a, CF Caspase 9 were from Cell Signaling Technology, Beverly, MA; Caspase7, Caspase2, Mcl-1, XIAP were from BD Pharmingen (Transduction Laboratories), Lexington, KY; PARP (C-2–10), Smac was from Upstate Biotechnology, Lake Placid, NY; Caspase-8 was from

Alexis, San Diego, CA; Tubulin was from Oncogene, San Diego, CA. Actin was purchased from sigma, MO. Bcl-2 was from Dako, CA. Caspase 4 was obtained from Stressgene Bioreagents, Ann, MI. Secondary antibodies were obtained from KPL Protein Research Products, Gaithersburg, MD, USA.

ROS Generation Analysis

Cells were suspended into 24-well cell culture plates for 24 hours. Two hours prior to drug treatment, antioxidants MnTBAP or N-Acetyl-L-cysteine were added to the appropriate wells, and cells were collected, incubated with ROS dye for 20 mins in the dark at room temperature, and analyzed for ROS generation on the cytofluorometer 30 minutes and 3 hours after drug treatment.

Animal Studies

Animal studies were performed in NIH-III nude mice procured from Charles River, Wilmington, MA, USA. $10x10^6$ SUDHL4 cells were pelleted by centrifugation, washed twice with 1X PBS and re-suspended in 75 ul of PBS. Cells were injected subcutaneously into the right flank. In order to improve the tumor take rate, cells were extracted from previously formed tumor (designated as SUDHLT cells) and grown for subsequent injection. Mice were checked two to three times a week for appearance of tumors. Once the tumors were visible, mice were grouped having at least 3 to 4 tumors in each group with approximately equal mean tumor volume. Mice were treated with various concentrations of carfilzomib via tail vein injection twice a week (1^{st}, 2^{nd}, 8^{th}, 9^{th}

days etc) and vorinostat was administered by IP injection thrice a week (1^{st}, 2^{nd}, 3^{rd} , 8^{th}, $9^{th,}$ 10^{th} days etc). Tumor volume was measured 2 to 3 times a week with the help of a caliper using the following formula

$$\text{Tumor Volume (CC)} = \frac{\text{Length (mm) X Width (mm)}^2}{2}$$

Mice were sacrificed once tumors were bigger than 2000 cc. Side effects of tumor growth and treatment was closely monitored by premature death of mice, loss of weight, and behavioral change such as lack of movement, etc.

Formulation of carfilzomib and vorinostat for in vivo studies

Vorinostat was originally dissolved in DMSO and stored in -80^0C in small aliquots. Finally it is diluted in 1:1PEG400 and sterile water to have final composition of 10% DMSO, 45% PEG400, 45% water. Volume of the treatment to each mouse with was restricted to 100ul or less. Stock carfilzomib was prepared with 10% sulfobutylether betacyclodextrin in 10mM citrate buffer pH 3.5 (vehicle) at the concentration 2mg/mL and stored at -80^0C. Stocks carfilzomib solution was diluted with vehicle every day for treatment at various doses

NF-κB Activity

Nuclear protein was extracted using Nuclear Extract Kit (Active Motif) and NF-κB activity was determined by using an enzyme linked immunosorbent assay (ELISA)

Kit TransAM NF-κB p65 Transcription Factor Assay Kit (Active Motif), according to manufacturer's instructions. Briefly, the activated form of NF-κB that is present in nuclear extracts was detected by using an anti-p65 specific antibody that recognizes the NF-κB bound to a consensus DNA oligonucleotide immobilized in a 96-well plate. Addition of a secondary antibody conjugated to horseradish peroxidase provides sensitive readout by spectrophotometry.

Cell Cycle Analysis

Cells ($4x10^6$ million/sample) were treated with varying drug concentrations, pelleted in 15 mL tubes, washed with PBS, and fixed in cold methanol and PBS at a ratio of 1 mL PBS to 3 mL methanol. Cells were stored in -20 C at least for 24 hrs. Cells were harvested for analysis and washed twice with ice cold PBS. Cells subsequently stained by 500 ul of 50ug/ml propidium Iodide for 30 minutes and accrued by flow cytometry. Individual cells population in each phage was determined with Modfit software.

Collection of S-100 fraction

Cells were harvested after drug treatment by centrifugation at 600 x *g* for 10 min at 4°C. Cell pellets were washed once with ice-cold PBS and resuspended in five volumes of buffer A [20 mM HEPES-KOH (pH 7.5), 10 mM KCl, 1.5 mM $MgCl_2$, 1 mM sodium EDTA, 1 mM sodium EGTA, 1 mM DTT, 0.1 mM phenylmethylsulfonyl fluoride, and 250 mM sucrose]. After being chilled for 30 min on ice, the cells were disrupted by 15 strokes of a glass homogenizer. The homogenate was centrifuged twice to remove

unbroken cells and nuclei (750 x *g*, 10 min, 4°C). S-100 fractions (supernatants) were then obtained by centrifugation at 100,000 x *g*, 60 min at 4°C. All steps were performed on ice or 4°C.

Statistical Analysis

The significance of differences between experimental conditions was determined using the two-tailed Student t test. Characterization of synergistic and antagonistic interactions was performed using Median Dose Effect analysis in conjunction with a commercially available software program (CalcuSyn, Biosoft, Ferguson, MO).

RESULTS

Proteasome inhibitors and HDAC inhibitors interact synergistically in a variety of DLBCL cell types

Interactions between the proteasome inhibitor carfilzomib and HDAC inhibitors vorinostat and SBHA were assessed in SUDHL16 and SUDHL4 cells, which are both GC subtype, as well as OCI-Ly10 cells, which are the ABC subtype. Individual exposures to low concentrations of carfilzomib and vorinostat for 16-24 hours induced limited lethality (e.g. 15-20% cell death). Combined exposure for 16-24 hours however, resulted in a marked increase in cell death, e.g. ~70-75% (Figure 1A), with CI values less than 1.0 by Median Dose effect analysis denoting synergism (Figure 1B).

To determine whether these findings are limited to carfilzomib and vorinostat, similar experiments were performed with SBHA, a commercially available HDAC inhibitor. Our results indicate that interactions between proteasome inhibitors and HDAC inhibitors are not restricted to carfilzomib and vorinostat (Figure 1A). Experiments performed with another HDAC inhibitor MS-275 resulted in similar synergistic interaction (data not shown). Sequential treatment of SUDHL16 cells with carfilzomib and vorinostat resulted in response similar to that of simultaneous treatment regardless of which drug was treated first (Figure 1C).

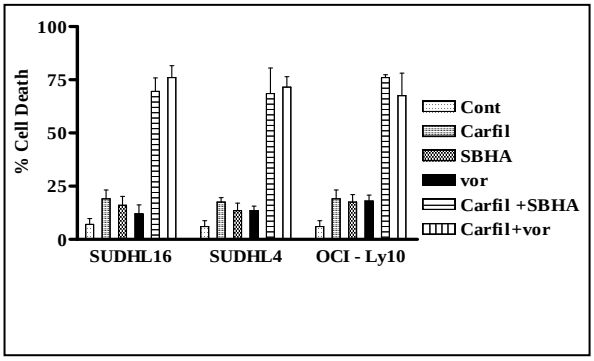

Fig. 1A: Proteasome inhibitors and HDAC inhibitors interact synergistically in a variety of DLBCL cells

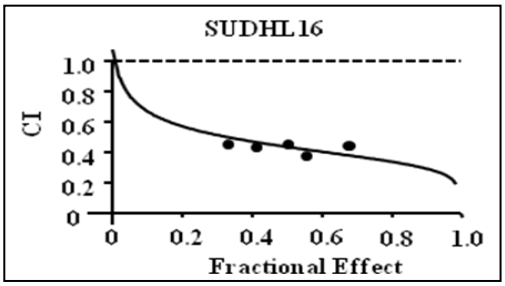

Fig. 1B: Median dose effect analysis for SUDHL16 cells

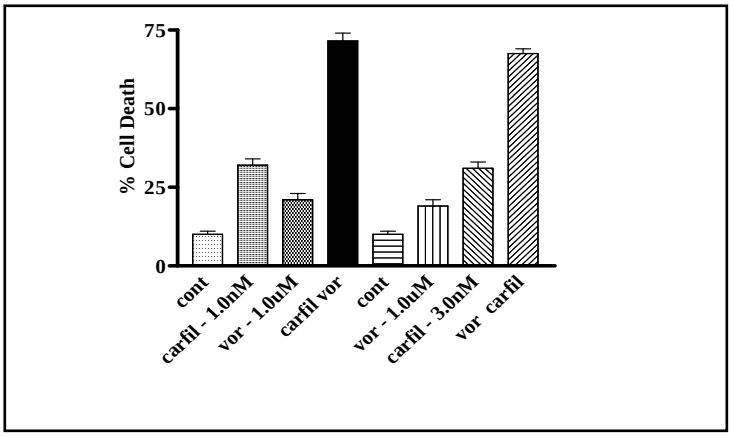

Fig. 1C: Sequential treatment with carfilzomib and vorinostat on SUDHL16 cells.

Figure 1 *Proteasome inhibitors and HDAC inhibitors interact synergistically in a variety of DLBCL cells*

(A). SUDHL16, SUDHL4, and OCI Ly10 cells we treated with minimally toxic concentrations of carfilzomib (2-5nM) ± vorinostat (0.75-2.0uM), or SBHA (30-60uM) for 24-48 hrs, after which cell death was monitored by 7AAD/$DiOC_6$ staining. (B). Fractional Effect values were determined by comparing results to those of untreated controls, and Median Dose Effect analysis was employed to characterize the nature of the interaction. Combination Index (C.I.) values less than 1.0 denote a synergistic interaction. (C). Sequential treatments were carried out in SUDHL16 cells, starting with pretreatment of either carfilzomib or vorinostat for 8hrs followed by the second drug for another 16 hours after which cell death was monitored by 7AAD/$DiOC_6$ staining.

Carfilzomib and vorinostat interact synergistically in DLBCL primary patient samples with minimal toxicity to normal cells

Interactions between proteasome inhibitors and HDAC inhibitors were assessed in primary DLBCL patient samples collected from patients to verify whether our findings of synergistic interaction of carfilzomib and vorinostat can be re-capitulated in primary cells. Individual exposure (10 hrs for samples presented in Figure 2A, 2B and 24 hrs for the sample presented in Figure 2C) to low concentrations of carfilzomib and vorinostat in ABC DLBCL cells (Figure 2A) induced limited lethality over control, while the combination produced a marked increase in lethality. Similar results were obtained in DLBCL cells from a patient who was not pretreated with any agents (Figure 2B), as well as in GC DLBCL cells from a relapsed patient albeit with higher doses, (Figure 2C). To determine whether this drug combination is toxic to normal cells, $CD34^+$ cells separated from bone marrow of a healthy donor were treated with 10 nM and 100 nM of carfilzomib and 1.5 μM of vorinostat. Both 10 nM and 100 nM concentrations or carfilzomib, as well as 1.5 μM vorinostat were minimally toxic to normal cells. Minimal toxicity was observed in cells treated with 10 nM carfilzomib and 1.5 μM vorinostat, and moderate toxicity was observed in cells treated with 100 nM carfilzomib and 1.5 μM vorinostat. However, no synergistic interaction was observed between these agents in these cells (Figure 2D).

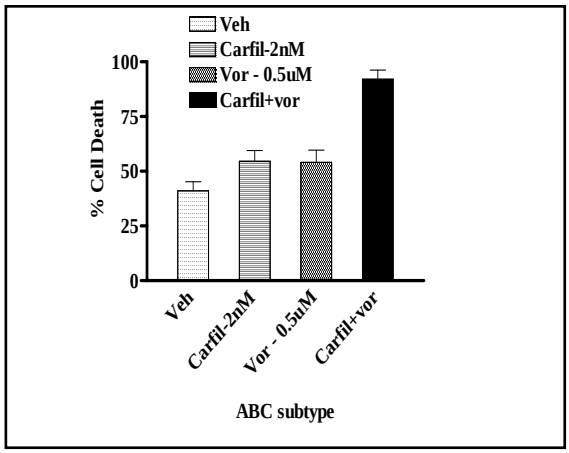

Fig. 2A

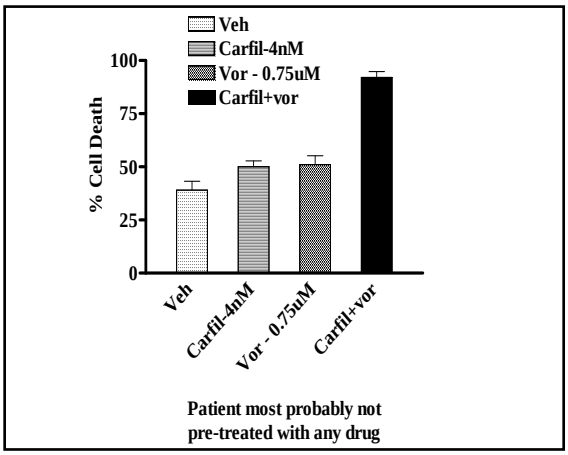

Fig. 2B

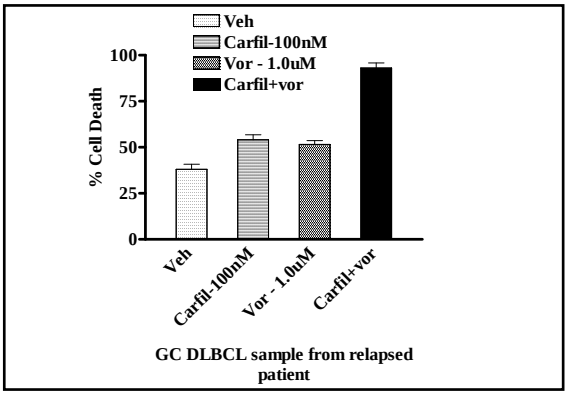

Fig. 2C. 07-109-V015: Patient was previously treated with CD20 antibody and relapsed. The current phenotype is CD5+19+20-. The original diagnosis was consistent with germinal center.

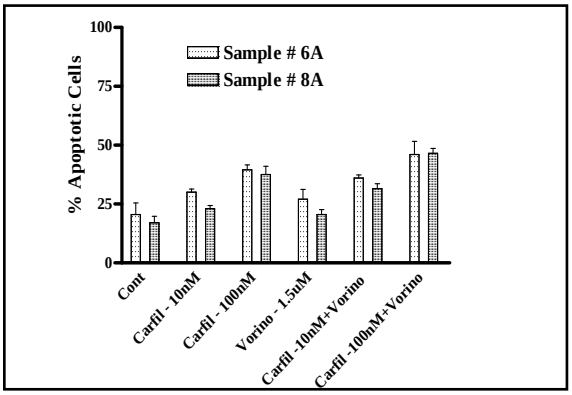

Fig. 2D. Normal CD34$^+$ cells were treated with 10 nM and 100 nM carfilzomib and 1.5 μM vorinostat.

Figure 2: *Carfilzomib and vorinostat also interact synergistically in DLBCL primary patient samples*

(A-C) Primary cells obtained from patients as described in Methods and exposed to carfilzomib (2 - 100nM) and Vorinostat (0.5 -1.0μM) for 10 - 24 hrs. The percentage of apoptotic cells was determined by Annexin V/PI staining and flow cytometry, and the percentage of viable cells in each sample was normalized to controls. (D) Normal CD34$^+$ cells were exposed to similar treatments.

Combined exposure of DLBCL cells to carfilzomib and vorinostat induces mitochondrial injury, caspase activation in association with marked JNK activation and induction of DNA damage

Treatment of SUDHL16 (a GC type DLBCL cells) for 14 hours with minimally toxic concentrations of carfilzomib and vorinostat resulted in a pronounced increase in activation of caspases-3, -8, -9 as well as release of mitochondrial pro-apoptotic proteins cytochrome c and SMAC (Figure 3A). Similar results were obtained with other DLBCL lines (e.g. SUDHL4; data not shown).

Effects of the combination were then examined in relation to MAPK signaling in SUDHL16 cells. While individual treatment of carfilzomib and vorinostat had little effect, combined treatment resulted in a dramatic increase in phosphorylation of the stress-related JNK kinase and that of its substrate c-Jun, as well as it's upstream target SEK1 (Fig 3B). In addition, carfilzomib alone induced p38 MAPK phosphorylation, but this was marginally enhanced by vorinostat (Figure 3B).

In view of evidence linking proteasome inhibitor lethality and induction of ER stress (54), effects of the combination were examined with respect to several ER stress markers. Whereas individual exposure exerted minimal effects, combined treatment resulted in modest but discernible increase in caspase-2 and a significant increase in caspase-4 cleavage/activation(Figure 3A). However we have also investigated the effect of carfilzomib and vorinostat on other ER related targets such as eIF2α phosphorylation, ATF4, PERK, etc which are considered to be the hallmark of ER stress induction, but we have not observed any major changes (data not shown).

There is a marked increase in the DNA damage marker γH2AX (Figure 3C). Also, we observe a notable decrease in the phosphorylation of AKT, as well as an increase in p21 and SOD2. Interestingly, this combination induced a marked increase in ERK phosphorylation (Figure 3D).

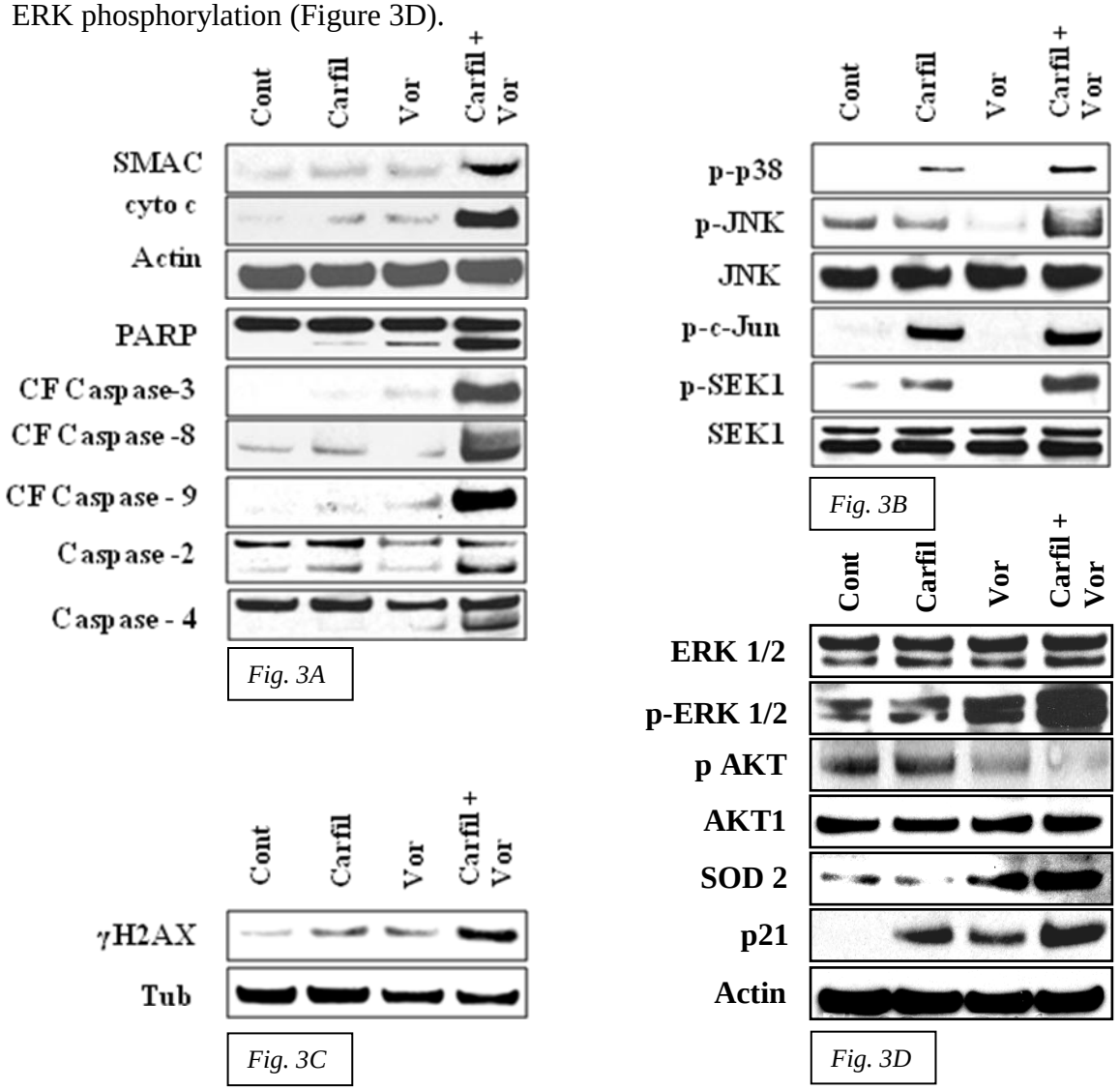

Figure 3: *Effects of carfilzomib and vorinostat on expression of relevant target proteins*

Cells were treated with minimally toxic concentrations of carfilzomib (2-5 nM) ± vorinostat (0.75-2.0 uM) for 24-48 hrs. After treatment cells were lysed, protein denatured, and subjected to Western blot analysis with the indicated primary antibodies. Blots were then stripped and reprobed with anti-actin or anti-tubulin to ensure equal loading and transfer of protein (20 μg in each lane). (A) markers of apoptosis, (B) MAPK pro-apoptotic pathway, (C) DNA damage markers, (D) other relevant targets.

Combined treatment of carfilzomib and vorinostat blocks the vorinostat induced activation of NF-κB.

It was previously reported that proteasome inhibitor bortezomib blocks the HDAC inhibitors induced Nf-κB activation which may be responsible, at least partly for their synergistic interaction. To whether similar phenomenon also involved in the interaction of carfilzomib and vorinostat, we treated SUDHL4 cells with minimally toxic concentrations of carfilzomib and vorinostat produced a significant decrease in NF-κB activity. Vorinostat alone resulted in a pronounced increase of NF-κB activity, which was significantly reduced in combination (Figure 4A). As expected, increasing the concentration of carfilzomib decreased NF-κB activity (Figure 4B).

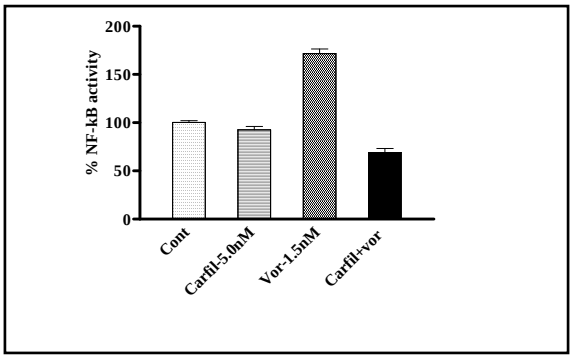

Fig. 4A. Co-administration of carfilzomib and vorinostat decreases NF-κB activity in SUDHL4

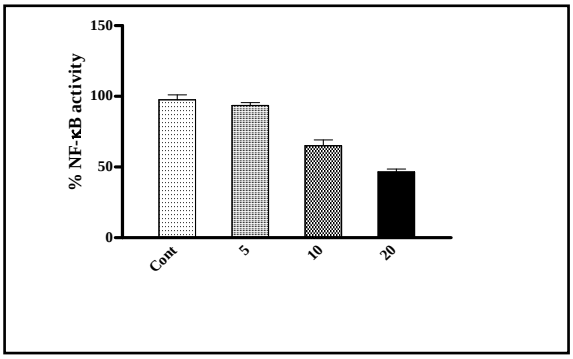

Fig. 4B. Increasing carfilzomib concentration decreases NF-κB activity in SUDHL4 cells.

Figure 4: *Effects of carfilzomib and vorinostat on NF-κB activity in SUDHL4 cells*

Nuclear protein was extracted using Nuclear Extract Kit (Active Motif) and NF-κB activity was determined by using an enzyme linked immunosorbent assay (ELISA) Kit TransAM NF-κB p65 Transcription Factor Assay Kit (Active Motif), as described in Methods. (A) Vorinostat alone increases NF-κB activity, which is subsequently blocked by co-administration of carfilzomib. (B) Increasing concentrations of carfilzomib alone decreases NF-κB activity.

Enhanced JNK activation plays a significant functional role in carfilzomib/vorinostat lethality in DLBCL cells.

To gain insights into the functional role of JNK activation in lethality of carfilzomib and vorinostat a genetic approach was employed. ShRNA knockdown of JNK1 (Figure 5A) in SUDHL 16 cells significantly diminished carfilzomib/vorinostat-mediated apoptosis (Fig 5B). It is consistent with other published results and suggests that JNK activation plays a functional role in the activity of this drug regimen.

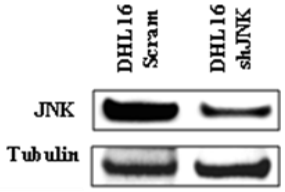

Fig. 5A. Western blot showing extent of JNK1 downregulation

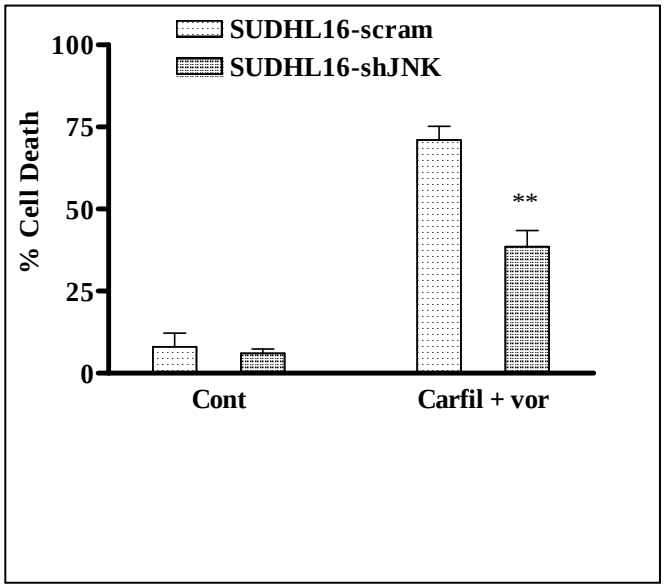

Fig. 5B. Downregulation of JNK1 by shJNK significantly decreases apoptosis in SUDHL16 cells.

Figure 5: *Enhanced JNK activation plays a significant functional role in carfilzomib/vorinostat lethality in DLBCL cells*

SUDHL16 cells were stably transfected with JNK shRNA or vectors encoding a scrambled sequence were exposed to 3.0 nM carfilzomib and 0.75 μM vorinostat. After 24 hr of drug exposure, apoptotic cells were monitored by 7AAD and $DiOC_6$ staining and flow cytometry. (A) Effect of JNK1 knockdown on carfilzomib/vorinostat lethality. (B) Western blot showing extent of JNK1 suppression. For (B) ** sigmificantly lower than values for empty vector controls; $p < 0.05$

Carfilzomib and vorinostat induced synergistic lethality involves ROS generation in SUDHL16 cells

Since proteasome inhibitor and HDAC inhibitors are known to induce oxidative stress (62,63), we further studied whether combined treatment of carfilzomib and vorinostat can further induce ROS generation when treated with sub-lethal concentration. Exposure of SUDHL16 cells (3 hr) to 3.0 nM carfilzomib and 0.75 μM vorinostat resulted in a marked increase in ROS generation, which was significantly reduced by co-administration of the antioxidant MnTBAP (Figure 6A). Co-administration of the antioxidant MnTBAP resulted in a significant decrease in cell death (Figure 6B). Co-administration with MnTBAP also significantly reduced caspase-3 activation as well as JNK phosphorylation (Figure 6C), both indicative of reduced cell death.

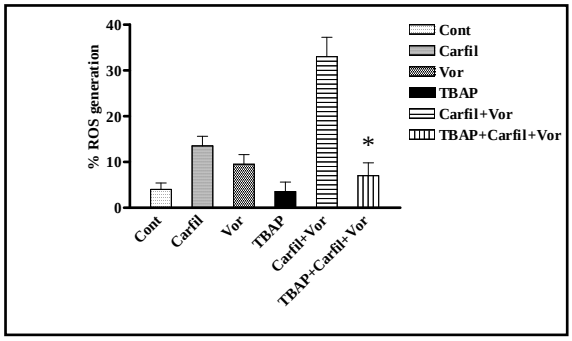

Fig. 6A. Incubation with MnTBAP for 3 hrs prior to treatment significantly reduces ROS generation.

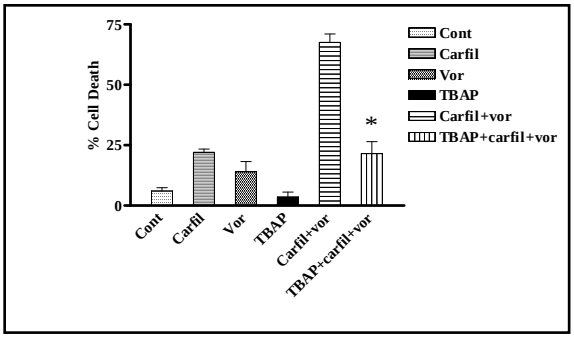

Fig. 6B. Blocking ROS generation significantly reduces cell death.

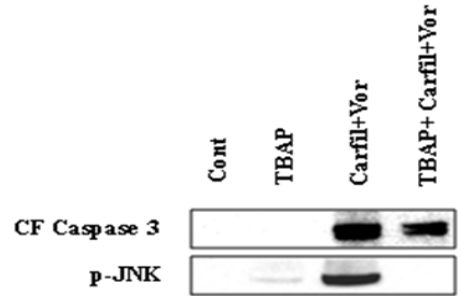

Fig. 6C

Figure 6: *Carfilzomib/vorinostat lethality involves ROS generation in DLBCL cells*

(A) SUDHL16 cells (preteated with or without 5 mM MnTBAP for 3 hrs) were exposed to 3.0 nM carfilzomib ± 0.75 μM vorinostat for 4 hrs. At the end of the drug exposure, ROS generation was monitored via flow cytometry as described in Methods. (B) SUDHL16 cells (preteated with or without 75 mM MnTBAP for 3 hrs) were exposed to 3.0 nM carfilzomib ± 0.75 μM vorinostat for 24 hrs. At the end of the drug exposure, cell death was monitored by 7AAD/$DiOC_6$ staining as described in Methods. (C) SUDHL16 cells (preteated with or without 75 mM MnTBAP for 3 hrs) were exposed to 3.0 nM carfilzomib ± 0.75 μM vorinostat for 24 hrs. At the end of the drug exposure, cells were harvested, lysed, protein denatured, and subjected to Western blot analysis with the indicated primary antibodies.

Co-administration of carfilzomib and vorinostat causes cell cycle arrest in the G2-M phase in both GC and ABC DLBCL subtypes

To gain insight into whether or not this drug combination causes cell cycle arrest, we analyzed the cell cycle in both GC and ABC subtypes. Single treatments with minimally toxic concentrations of carfilzomib (7.5 nM) and vorinostat (1.5 μM) in OCI-Ly10 ABC type DLBCL cells resulted in minimal cell cycle arrest in the G2-M phase, while combinational treatments resulted in a marked increase in G2-M arrest (Figure 7A). Parallel experiment was carried out in SUDHL4 cells, which are of the GC subtype, and while minimally toxic concentrations of carfilzomib (5.0 nM) and vorinostat (1.5 μM) resulted in minimal G2-M arrest, combination therapy resulted in a very large increase in G2-M arrested cells (Figure 7B).

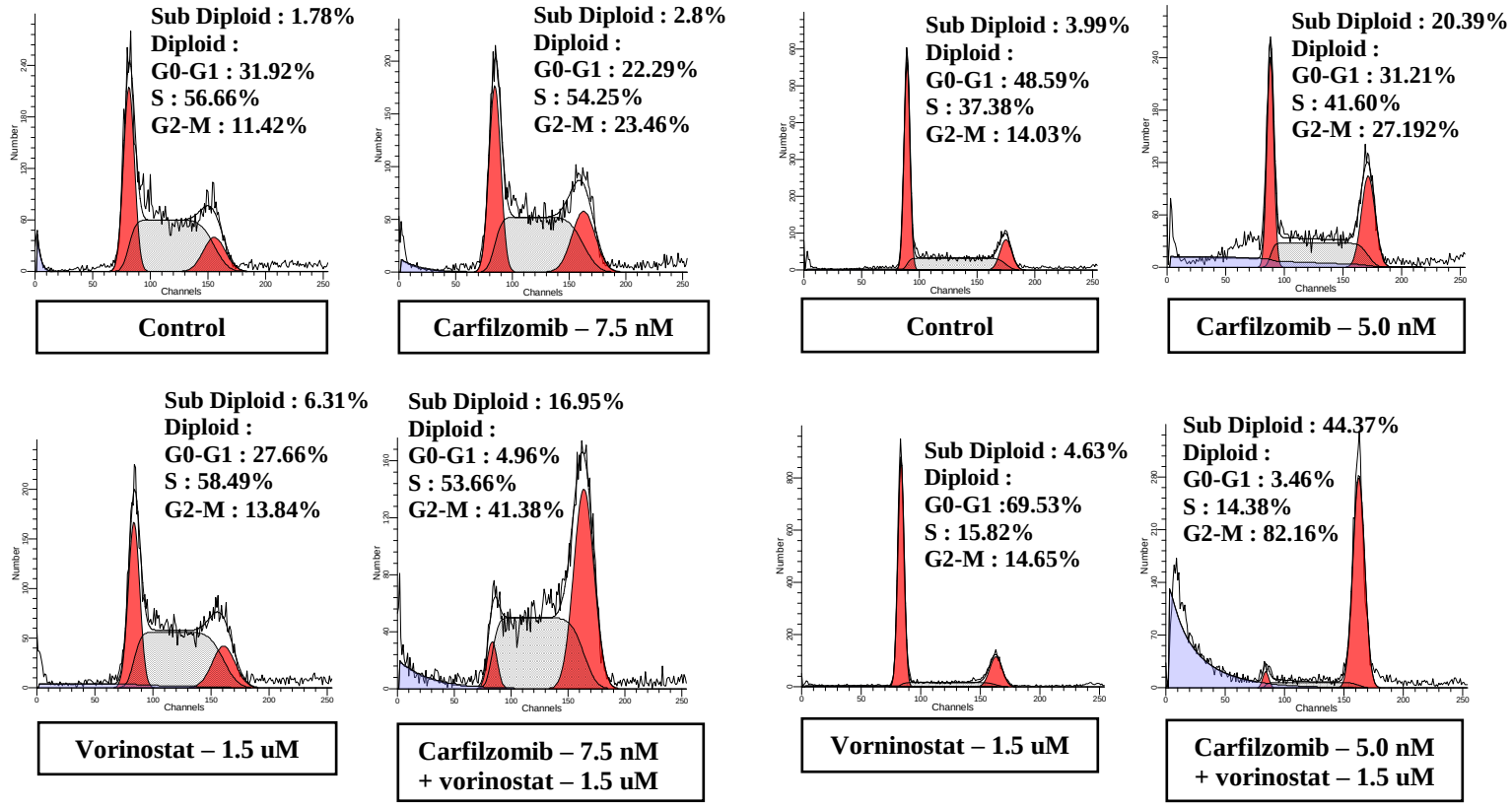

Fig. 7A. Co-administration of carfilzomib and vorinostat in OCI Ly10 cells results in marked G2-M arrest

Fig. 7B. Co-administration of carfilzomib and vorinostat in SUDHL4 cells results in striking G2-M arrest

Figure 7: *Co-administration of carfilzomib and vorinostat results in G2-M cell cycle arrest in both ABC and GC DLBCL subtypes.*

OCI Ly10 and SUDHL4 cells were treated with carfilzomib and vorinostat as indicated. After treatment, cells were collected, fixed in ice cold methanol at a ratio of 1 mL PBS to 3 mL methanol, and analyzed by flow cytometry as described in Methods. (A) OCI Ly10. (B) SUDHL4.

There is minimal cross-resistance to carfilzomib in bortezomib resistant DLBCL lymphoma cells, and is overcome by a synergistic combined treatment of carfilzomib and vorinostat.

Since patients treated with bortezomib often relapse and become resistant to their treatment, we examined whether or not there is cross resistance to carfilzomib in bortezomib resistant DLBCL cells. To determine whether similar interactions might occur in cells resistant to bortezomib, SUDHL16 and Raji cells that had been adapted to grow in the presence of bortezomib were employed. These cells (e.g. SUDHL16-10BR, Raji-20BR) were maintained in the presence of 10nM and 20nM of bortezomib respectively without any impact on cell growth or viability. These cells express equivalent CD20 expression, compared to their parental counterparts, confirming their B-cell origin (64). To rule out the possibility that bortezomib resistance might reflect development of the multi-drug resistance (MDR) phenotype, Pgp expression was monitored by flow cytometry. No increase in Pgp expression was observed in either resistant cell line, nor did cross-resistance to VP-16, a Pgp substrate, occur (data not shown).

Both Raji-20BR and SUDHL16-10BR cells exhibited minimal cross resistance to carfilzomib (Figure 8A-B). This cross-resistance is easily overcome via combinational treatments using minimally toxic concentrations of carfilzomib (5-15 nM) as well as vorinostat (1.5-2.0 μM) and SBHA (40-60 μM) in both SUDHL16-10BR and Raji-20BR cell lines, as combined exposure for 16-24 hours resulted in a marked increase in cell

death, e.g. ~65-75% (Figure 8C). CI values less than 1.0 by Median Dose effect analysis denoting synergism (Figure 8D).

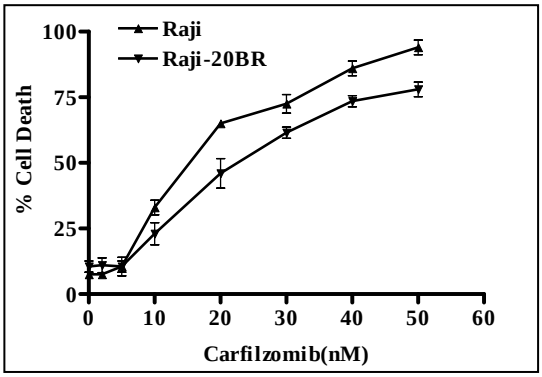

Fig. 8A. Marginal cross-resistance to carfilzomib is observed in Raji cells resistant

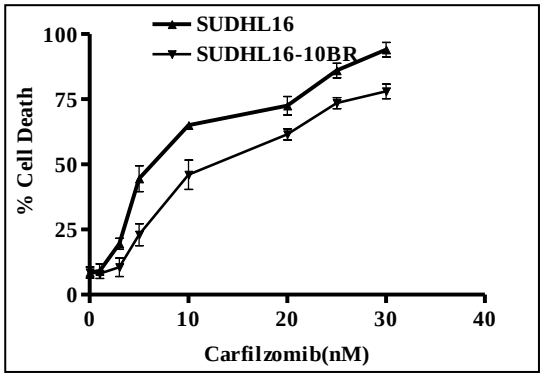

Fig. 8B. Marginal cross-resistance to carfilzomib is observed in SUDHL16 cells resistant to 20nM bortezomib.

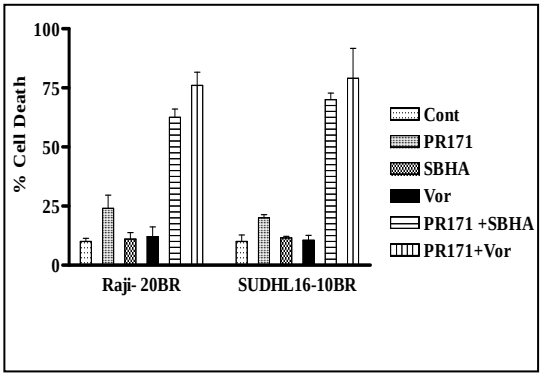

Fig. 8C. Bortezomib-induced cross-resistance to carfilzomib is overcome in both Raji-20BR and SUDHL16-10BR

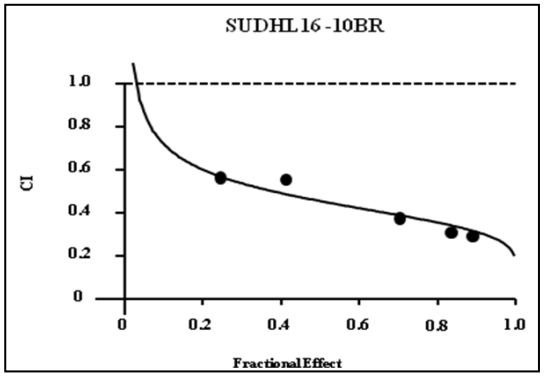

Fig. 8D. Combination index values less than 1.0 indicate synergy

Figure 8: *Minimal cross-resistance to carfilzomib was observed in bortezomib resistant DLBCL lymphoma cells, and is overcome by co-administration of carfilzomib and vorinostat.*

(A-B) Raji-20BR and SUDHL16-10BR were treated with increasing concentrations of carfilzomib as indicated, and cell death was monitored by 7AAD/DiOC$_6$ staining. (C) SUDHL16-10BR and Raji-20BR cells were treated with minimally toxic concentrations of carfilzomib (5-15nM) ± vorinostat (1.5-2.0μM), or SBHA (40-60μM) for 24-48 hrs, after which cell death was monitored by 7AAD/DiOC$_6$ staining. (D) Fractional Effect values were determined by comparing results to those of untreated controls, and Median Dose Effect analysis was employed to characterize the nature of the interaction. Combination Index (C.I.) values less than 1.0 denote a synergistic interaction.

Co-administration of carfilzomib and vorinostat induce in vivo tumor growth reduction in SUDHL4T cells

We have further investigated the antitumor activity of carfilzomib and vorinostat in BNX mice (NIH-III) bearing established human tumor xenografts derived from SUDHL4T cells as described in methods. First we have evaluated the antitumor effect of carfilzomib and vorinostat alone against this SUDHL4T tumor cells. Carfilzomib was administered in doses of 0.5 mg/Kg, 2.0 mg/Kg, and 3.0 mg/Kg and we have observed dose dependent reduction of tumor growth starting with 2.0 mg/Kg (Figure (9A & 9B). We have also observed that treatment with vorinostat (75 mg/Kg) also induced significant tumor growth reduction (Figure 9C). Based on the results of single drug response of carfilzomib and vorinostat, we have performed two separate set of experiments with the following dosing

Experiment -1 carfilzomib – 1.5 mg/kg & vorinostat – 40 mg/kg

Experiment -2 carfilzomib – 3.0 mg/kg & vorinostat – 60 mg/kg

Each group of the experiment has four groups of mice, with each group having 3-4 mice treated. One group of mice was treated with vehicle, where as two groups were treated with either carfilzomib or vorinostat alone and remaining groups was treated with combined dose of carfilzomib and vorinostat. Based on the results of four weeks of dosing, we have observed that co-treatment of carfilzomib and vorinostat have induced significantly more growth reduction of tumors in comparison to the single drug treatment (Figure 9D & 9E). However we have not observed any tumor regression in any of the mice.

Fig. 9A. Photographs taken of mice treated with increasing doses of carfilzomib

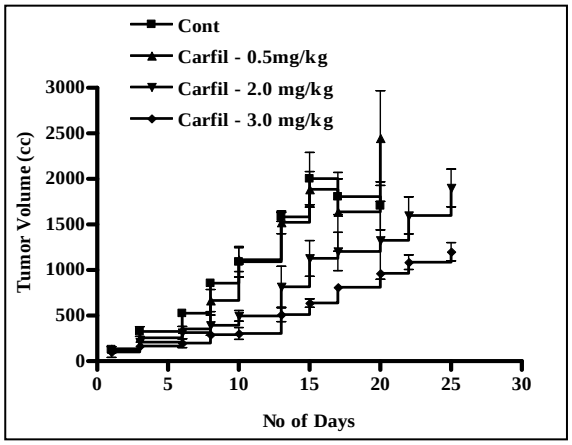

Fig. 9B. Tumor volumes in mice treated with increasing concentrations of carfilzomib.

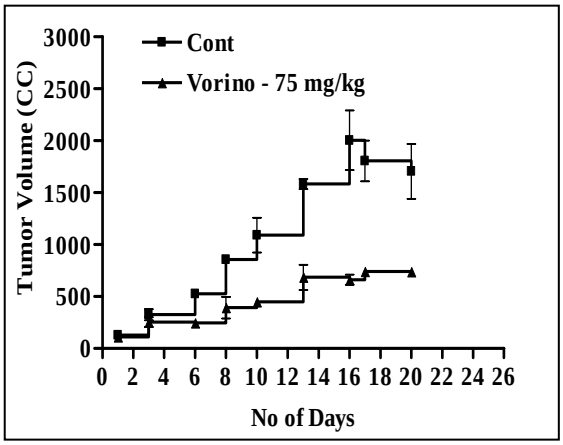

Fig. 9C. Tumor volumes in mice treated with 75 mg/Kg of vorinostat

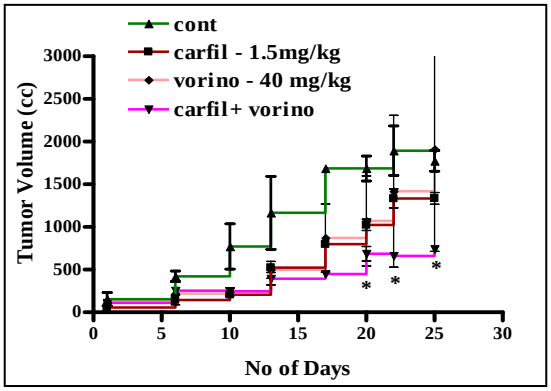

Fig. 9D. Tumor volumes in mice treated with 1.5 mg/Kg carfilzomib and 40 mg/Kg vorinostat

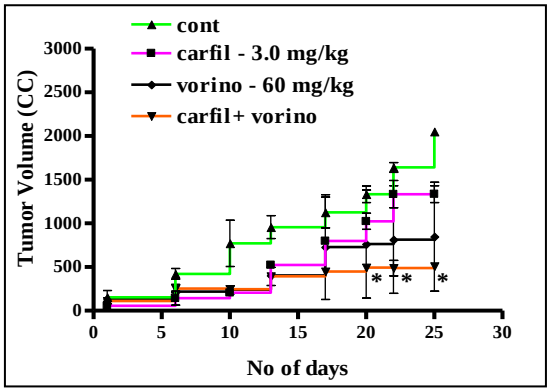

Fig. 9E. Tumor volumes in mice treated with 3.0 mg/Kg carfilzomib and 60 mg/Kg vorinostat

Figure 9: *Carfilzomib and vorinostat cause tumor growth reduction in SUDHL4T cells*

NIH-III nude mice were treated with carfilzomib ± vorinostat as previously described in Methods, at the indicated concentrations. (A) Photographs of single treatments with carfilzomib. (B-C) Tumor volumes after single treatments with carfilzomib and vorinostat at the indicated concentrations. (D-E) Tumor volumes after co-administration of carfilzomib and vorinostat as described in Methods, at the indicated concentrations. For (A) & (B) * = significantly grater than values for carfilzomib and vorinostat treatment alone; $p < 0.05$

DISCUSSION

Since recent reports of clinical trials of Bortezomib in diffuse large b-cell lymphoma patients have demonstrated poor clinical response (3,65), development of alternative therapeutic options based on new generation of proteasome inhibitors may be an attractive choice. Second generation of proteasome inhibitors, i.e. carfilzomib which has been reported to have improved efficacy to bortezomib, can logically be used to develop a drug regimen to treat DLBCL patients.

The present evidence extends previous findings that HDAC inhibitors activate the NF-κB survival pathways (59), whereas proteasome inhibitors block this activation (15). Bortezomib and vorinostat have also been shown to interact synergistically in many cancer cell types, including hematologic malignancies as well as solid tumors, and this study extends these finding to the second generation proteasome inhibitor carfilzomib and DLBCL cells. There is clear synergy in combinations of carfilzomib and vorinostat in diffuse large B-cell lymphoma cell lines and patient samples. Several mechanisms appear to be playing a role in this combined lethality, including mitochondrial outer membrane permeabilization, caspase activation, ROS generation, and cell cycle arrest.

Recently, microarray analyses performed on untreated DLBCL has lead to the identification of two main sub-types, germinal center (GC-DLBCL), and activated B-cell (ABC-DLBCL). Both have a distinct gene expression profile, characteristic of either normal germinal center b-cells or activated blood memory B-cells (4). The germinal

center-like subgroup is correlated with a significantly better prognosis in comparison with the activated B-cell like subgroup (4), and the 5-year survival rate of both is 59% and 30% respectively (5). A third subgroup is comprised of cases that do not express the genetic profile of either the ABC or GC subgroups (4) was not the subject of this study. Synergistic interactions with carfilzomib and vorinostat on cell death were observed in both GC and ABC DLBCL cells, and similar results were obtained with other HDAC inhibitors such as SBHA and MS-275. Therefore these results are applicable to other classes of HDAC inhibitors, and are not restricted to vorinostat alone. Combination-induced cell death did not appear to depend on whether the treatment was sequential or consecutive, as the results for both studies were very similar. Similar synergistic interactions were also observed in both the ABC and GC subgroups of patient samples, including samples from relapsed patients.

For any cancer treatment regimen to be viable and effective, it must not be overly toxic to normal cells. It is important to note that no synergistic interaction with the two compounds was observed in $CD34^+$ normals, indicating that this treatment regimen presents minimal toxicity to untransformed cells.

The stress-related MAPK JNK is known to exert a pro-apoptotic role in cellular responses to diverse noxious stimuli (66). JNK activation has been implicated in proteasome inhibitor lethality in both hematopoietic (40,61) and non-hematopoietic malignant cells (67). Our results show significant phosphorylation of JNK, as well as phosphorylation of its upstream target SEK1 and its downstream target c-Jun. To

confirm the functional role of JNK in the combinational regimen of carfilzomib and vorinostat, a genetic shRNA knockdown of JNK was employed. This approach resulted in a significant reduction in cell death, as well as caspase-3 activation and JNK phosphorylation (data not shown), indicating that the JNK MAPK pathway is playing a role in carfilzomib and vorinostat combination induced apoptosis.

To determine the effect of the combination regimen on various relevant target proteins, we performed western analyses on whole cell lysates. Our data shows significant pro-apoptotic caspase activation, marked increase in the oxidative stress marker SOD2, marked decrease in AKT, and marked increase of the DNA damage marker γH2AX. Interestingly, there was a large increase in ERK (p44/42) phosphorylation, indicating that the pro-survival pathway is being activated even in combination.

In light of evidence that proteasome inhibitors and HDAC inhibitors both induce ROS generation and oxidative stress (40,51), we looked to see whether this event plays a role in apoptosis as a result of combinational treatment with the two compounds. Single treatments of SUDHL16 cells with either carfilzomib or vorinostat resulted in a moderate increase in ROS generation, however combining the two compounds resulted in a very profound ROS increase as well as cell death. Co-administration of the MnTBAP antioxidant with carfilzomib and vorinostat significantly blocked ROS generation and resulted in a significant reduction of cell death. In addition, co-administration of MnTBAP together with carfilzomib and vorinostat resulted in a marked decrease in the activation of the apoptotic effecter caspase-3, a phenomenon known to play an important

role in mediating the cellular response to oxidative injury (51,68). A profound reduction in the phosphorylation of JNK, part of the stress-related pro-apoptotic pathway (66) was also observed in the combined regimen of carfilzomib and vorinostat. Finally, NF-κB is known to play a major protective role in cells undergoing oxidative damage (32), thus the carfilzomib/vorinostat regimen may trigger cell death through multiple mechanisms, including ROS generation as well as a reduction in NF-κB activation. These results provide support for the notion that disruption of the cellular redox state may represent an important mechanism underlying DLBCL cell death when exposed to these compounds, both alone and in combination.

Combined exposure of both GC and ABC DLBCL cells was associated with cell cycle perturbation. Minimally toxic concentrations of vorinostat alone had little effect on cell cycle arrest, while carfilzomib alone resulted in a slight increase cells population in G2-M phase. Combined treatments however resulted in profound increases of G2-M arrested cells. This evidence suggests that cell cycle arrest from a regimen combining carfilzomib and vorinostat may play a role carfilzomib and vorinostat mediated cell death. This is very much in accord with our finding that combined treatment of carfilzomib and vorinostat induces DNA damage as evident from the up regulation of γH2AX

The NF-κB pathway is known to play a crucial role in DLBCL cell survival (9), and the capacity of carfilzomib to inhibit the NF-κB pathway by blocking protesomal IκB degradation likely plays a key role in the activity of this agent against DLBCL cells. In accordance with this evidence, our findings show that increasing concentrations of

carfilzomib block activation of NF-κB. In accordance with evidence that HDAC inhibitors induce NF-κB activation (59), our studies show a profound increase in NF-κB activation in vorinostat-treated cells. Combined exposure of SUDHL4 cells to carfilzomib and vorinostat was associated in a very substantial decline in NF-κB activaty. These findings demonstrate a potential pathway for the synergy of carfilzomib and vorinostat.

Acquired resistance to treatment is always a concern in patients currently undergoing therapy, especially if the patient has relapsed. To address this concern, we examined whether or not there is cross resistance to carfilzomib in bortezomib resistant DLBCL cells. We generated SUDHL16 cells resistant to 10 nM bortezomib (SUDHL16-10BR), and Raji cells resistant to 20 nM bortezomib (Raji-20BR), with both lines having an 4-5 fold increase of LC50 than the parental cells. Both SUDHL16-10BR and Raji-20BR cells exhibited partial cross resistance to carfilzomib. Upon treatment of the resistant lines with a combined regimen of carfilzomib and vorinostat, we saw a profound synergistic response in both resistant cell lines, indicating that this combination regiment can be an attractive option in patients that developed resistant to other proteasome inhibitors.

In vivo studies are crucial to confirm the efficacy of this drug combination regimen. Our early *in vivo* studies were performed with single drug dosing by injecting NIH-III beige nude mice subcutaneously with SUDHL4 cells passaged from extracted tumors that developed in athymic nude mice, in order to determine the dose-response. These passaged cells were given the SUDHL4T designation. Our results indicated that

increasing concentrations of carfilzomib had a marked effect on the growth rate of SUDHL4T tumors, and a 75 mg/kg dose of vorinostat had a profound effect on tumor growth. Two experiments with combining carfilzomib and vorinostat were performed: the first used 1.5 mg/kg of carfilzomib and 40 mg/kg of vorinostat and the second used 3.0 mg/kg of carfilzomib and 60 mg/kg of vorinostat. Both combinations resulted in a decrease in tumor volume when compared to single drug treatments and the control, with the higher dose resulting in a slightly better effect. However, we have not seen any tumor regression in any of the experiments. These findings may suggest that animals should be treated for longer period of time, treatments should be performed more frequently, or the concentrations of drugs should be optimized further. Since we also observed a large increase in ERK phosphorylation induced by the combination of carfilzomib and vorinostat *in vitro*, it may be worthwhile to combine carfilzomib and vorinostat with a MEK inhibitor such as PD184352. It will also be interesting to see if we can improve the in-vivo efficiency by sequentially scheduling the drug treatment rather than administering the agents simultaneously.

In conclusion, our evidence supports the notion that combining the second-generation proteasome inhibitor carfilzomib with the HDAC inhibitor vorinostat presents a viable treatment option for both germinal center and activated B-cell type DLBCL. Cell death is mediated by various mechanisms, including ROS generation, cell cycle arrest, JNK activation, induction of DNA damage, and NF-κB inhibition. This regimen is effective in both cell lines as well as patient samples, and is able to overcome any cross

resistance to the first-generation proteasome inhibitor bortezomib. Finally, this combination shows promising results *in vivo* and requires further investigation for clinical development.

REFERENCES

2. Alizadeh AA, Eisen MB, Davis RE *et al.* (2000) Distinct types of diffuse large B-cell lymphoma identified by gene expression profiling. *Nature* **403**: 503-11.

3. Coiffier B, Lepage E, Briere J *et al.* (2002) CHOP chemotherapy plus rituximab compared with CHOP alone in elderly patients with diffuse large-B-cell lymphoma. *N.Engl.J.Med.* **346**: 235-42.

4. De Paepe P, Wolf-Peeters C (2007) Diffuse large B-cell lymphoma: a heterogeneous group of non-Hodgkin lymphomas comprising several distinct clinicopathological entities. *Leukemia* **21**: 37-43.

5. Bea S, Zettl A, Wright G *et al.* (2005) Diffuse large B-cell lymphoma subgroups have distinct genetic profiles that influence tumor biology and improve gene-expression-based survival prediction. *Blood* **106**: 3183-90.

6. Rosenwald A, Wright G, Chan WC *et al.* (2002) The use of molecular profiling to predict survival after chemotherapy for diffuse large-B-cell lymphoma. *N.Engl.J.Med.* **346**: 1937-47.

7. Huang JZ, Sanger WG, Greiner TC *et al.* (2002) The t(14;18) defines a unique subset of diffuse large B-cell lymphoma with a germinal center B-cell gene expression profile. *Blood* **99**: 2285-90.

8. Iqbal J, Sanger WG, Horsman DE *et al.* (2004) BCL2 translocation defines a unique tumor subset within the germinal center B-cell-like diffuse large B-cell lymphoma. *Am.J.Pathol.* **165**: 159-66.

9. Adams J (2004) The proteasome: a suitable antineoplastic target. *Nat.Rev.Cancer* **4**: 349-60.

10. Peters JM, Cejka Z, Harris JR, Kleinschmidt JA, Baumeister W (1993) Structural features of the 26 S proteasome complex. *J.Mol Biol.* **234**: 932-7.

11. Ciechanover A (1998) The ubiquitin-proteasome pathway: on protein death and cell life. *EMBO J.* **17**: 7151-60.

12. DeMartino GN, Slaughter CA (1999) The proteasome, a novel protease regulated by multiple mechanisms. *J.Biol.Chem.* **274**: 22123-6.

13. Kisselev AF, Akopian TN, Castillo V, Goldberg AL (1999) Proteasome active sites allosterically regulate each other, suggesting a cyclical bite-chew mechanism for protein breakdown. *Mol Cell* **4**: 395-402.

14. Benaroudj N, Zwickl P, Seemuller E, Baumeister W, Goldberg AL (2003) ATP hydrolysis by the proteasome regulatory complex PAN serves multiple functions in protein degradation. *Mol Cell* **11**: 69-78.

15. McConkey DJ, Zhu K (2008) Mechanisms of proteasome inhibitor action and resistance in cancer. *Drug Resist.Updat.* **11**: 164-79.

16. Pickart CM (2001) Ubiquitin enters the new millennium. *Mol Cell* **8**: 499-504.

17. Kaufman RJ (2002) Orchestrating the unfolded protein response in health and disease. *J.Clin.Invest* **110**: 1389-98.

18. Ron D (2002) Translational control in the endoplasmic reticulum stress response. *J.Clin.Invest* **110**: 1383-8.

19. Johnston JA, Ward CL, Kopito RR (1998) Aggresomes: a cellular response to misfolded proteins. *J.Cell Biol.* **143**: 1883-98.

20. Kawaguchi Y, Kovacs JJ, McLaurin A, Vance JM, Ito A, Yao TP (2003) The deacetylase HDAC6 regulates aggresome formation and cell viability in response to misfolded protein stress. *Cell* **115**: 727-38.

21. Kopito RR (2000) Aggresomes, inclusion bodies and protein aggregation. *Trends Cell Biol.* **10**: 524-30.

22. Fratta P, Engel WK, McFerrin J, Davies KJ, Lin SW, Askanas V (2005) Proteasome inhibition and aggresome formation in sporadic inclusion-body myositis and in amyloid-beta precursor protein-overexpressing cultured human muscle fibers. *Am.J.Pathol.* **167**: 517-26.

23. Hideshima T, Bradner JE, Wong J *et al.* (2005) Small-molecule inhibition of proteasome and aggresome function induces synergistic antitumor activity in multiple myeloma. *Proc.Natl.Acad.Sci.U.S.A* **102**: 8567-72.

24. Nawrocki ST, Carew JS, Pino MS *et al.* (2006) Aggresome disruption: a novel strategy to enhance bortezomib-induced apoptosis in pancreatic cancer cells. *Cancer Res.* **66**: 3773-81.

25. Karin M, Cao Y, Greten FR, Li ZW (2002) NF-kappaB in cancer: from innocent bystander to major culprit. *Nat.Rev.Cancer* **2**: 301-10.

26. Beg AA, Baltimore D (1996) An essential role for NF-kappaB in preventing TNF-alpha-induced cell death. *Science* **274**: 782-4.

27. Liu ZG, Hsu H, Goeddel DV, Karin M (1996) Dissection of TNF receptor 1 effector functions: JNK activation is not linked to apoptosis while NF-kappaB activation prevents cell death. *Cell* **87**: 565-76.

28. Van Antwerp DJ, Martin SJ, Kafri T, Green DR, Verma IM (1996) Suppression of TNF-alpha-induced apoptosis by NF-kappaB. *Science* **274**: 787-9.

29. Wang CY, Mayo MW, Baldwin AS, Jr. (1996) TNF- and cancer therapy-induced apoptosis: potentiation by inhibition of NF-kappaB. *Science* **274**: 784-7.

30. Karin M, Lin A (2002) NF-kappaB at the crossroads of life and death. *Nat.Immunol.* **3**: 221-7.

31. Wang CY, Cusack JC, Jr., Liu R, Baldwin AS, Jr. (1999) Control of inducible chemoresistance: enhanced anti-tumor therapy through increased apoptosis by inhibition of NF-kappaB. *Nat.Med.* **5**: 412-7.

32. Shi X, Dong Z, Huang C *et al.* (1999) The role of hydroxyl radical as a messenger in the activation of nuclear transcription factor NF-kappaB. *Mol Cell Biochem.* **194**: 63-70.

33. Inoue S, Browne G, Melino G, Cohen GM (2009) Ordering of caspases in cells undergoing apoptosis by the intrinsic pathway. *Cell Death.Differ.*

34. Wang CY, Mayo MW, Korneluk RG, Goeddel DV, Baldwin AS, Jr. (1998) NF-kappaB antiapoptosis: induction of TRAF1 and TRAF2 and c-IAP1 and c-IAP2 to suppress caspase-8 activation. *Science* **281**: 1680-3.

35. Lassus P, Opitz-Araya X, Lazebnik Y (2002) Requirement for caspase-2 in stress-induced apoptosis before mitochondrial permeabilization. *Science* **297**: 1352-4.

36. Hitomi J, Katayama T, Eguchi Y *et al.* (2004) Involvement of caspase-4 in endoplasmic reticulum stress-induced apoptosis and Abeta-induced cell death. *J.Cell Biol.* **165**: 347-56.

37. Varfolomeev EE, Schuchmann M, Luria V *et al.* (1998) Targeted disruption of the mouse Caspase 8 gene ablates cell death induction by the TNF receptors, Fas/Apo1, and DR3 and is lethal prenatally. *Immunity.* **9**: 267-76.

38. Adams J, Kauffman M (2004) Development of the proteasome inhibitor Velcade (Bortezomib). *Cancer Invest* **22**: 304-11.

39. Adams J, Behnke M, Chen S *et al.* (1998) Potent and selective inhibitors of the proteasome: dipeptidyl boronic acids. *Bioorg.Med.Chem.Lett.* **8**: 333-8.

40. Fribley A, Zeng Q, Wang CY (2004) Proteasome inhibitor PS-341 induces apoptosis through induction of endoplasmic reticulum stress-reactive oxygen species in head and neck squamous cell carcinoma cells. *Mol Cell Biol.* **24**: 9695-704.

41. Papandreou CN, Daliani DD, Nix D *et al.* (2004) Phase I trial of the proteasome inhibitor bortezomib in patients with advanced solid tumors with observations in androgen-independent prostate cancer. *J.Clin.Oncol.* **22**: 2108-21.

42. Papandreou CN, Logothetis CJ (2004) Bortezomib as a potential treatment for prostate cancer. *Cancer Res.* **64**: 5036-43.

43. Richardson PG, Barlogie B, Berenson J *et al.* (2003) A phase 2 study of bortezomib in relapsed, refractory myeloma. *N.Engl.J.Med.* **348**: 2609-17.

44. Demo SD, Kirk CJ, Aujay MA *et al.* (2007) Antitumor activity of PR-171, a novel irreversible inhibitor of the proteasome. *Cancer Res.* **67**: 6383-91.

45. Kuhn DJ, Chen Q, Voorhees PM *et al.* (2007) Potent activity of carfilzomib, a novel, irreversible inhibitor of the ubiquitin-proteasome pathway, against preclinical models of multiple myeloma. *Blood* **110**: 3281-90.

46. de Ruijter AJ, van Gennip AH, Caron HN, Kemp S, van Kuilenburg AB (2003) Histone deacetylases (HDACs): characterization of the classical HDAC family. *Biochem.J.* **370**: 737-49.

47. Wade PA (2001) Transcriptional control at regulatory checkpoints by histone deacetylases: molecular connections between cancer and chromatin. *Hum.Mol Genet.* **10**: 693-8.

48. Ito K, Barnes PJ, Adcock IM (2000) Glucocorticoid receptor recruitment of histone deacetylase 2 inhibits interleukin-1beta-induced histone H4 acetylation on lysines 8 and 12. *Mol Cell Biol.* **20**: 6891-903.

49. Sengupta N, Seto E (2004) Regulation of histone deacetylase activities. *J.Cell Biochem.* **93**: 57-67.

50. Lindemann RK, Newbold A, Whitecross KF *et al.* (2007) Analysis of the apoptotic and therapeutic activities of histone deacetylase inhibitors by using a mouse model of B cell lymphoma. *Proc.Natl.Acad.Sci.U.S.A* **104**: 8071-6.

51. Pei XY, Dai Y, Grant S (2004) Synergistic induction of oxidative injury and apoptosis in human multiple myeloma cells by the proteasome inhibitor bortezomib and histone deacetylase inhibitors. *Clin.Cancer Res.* **10**: 3839-52.

52. Martinez-Iglesias O, Ruiz-Llorente L, Sanchez-Martinez R, Garcia L, Zambrano A, Aranda A (2008) Histone deacetylase inhibitors: mechanism of action and therapeutic use in cancer. *Clin.Transl.Oncol.* **10**: 395-8.

53. Bolden JE, Peart MJ, Johnstone RW (2006) Anticancer activities of histone deacetylase inhibitors. *Nat.Rev.Drug Discov.* **5**: 769-84.

54. Minucci S, Pelicci PG (2006) Histone deacetylase inhibitors and the promise of epigenetic (and more) treatments for cancer. *Nat.Rev.Cancer* **6**: 38-51.

55. Richon VM, Emiliani S, Verdin E *et al.* (1998) A class of hybrid polar inducers of transformed cell differentiation inhibits histone deacetylases. *Proc.Natl.Acad.Sci.U.S.A* **95**: 3003-7.

56. Crump M, Coiffier B, Jacobsen ED *et al.* (2008) Phase II trial of oral vorinostat (suberoylanilide hydroxamic acid) in relapsed diffuse large-B-cell lymphoma. *Ann.Oncol.* **19**: 964-9.

57. Kelly WK, O'Connor OA, Krug LM *et al.* (2005) Phase I study of an oral histone deacetylase inhibitor, suberoylanilide hydroxamic acid, in patients with advanced cancer. *J.Clin.Oncol.* **23**: 3923-31.

58. O'Connor OA, Heaney ML, Schwartz L *et al.* (2006) Clinical experience with intravenous and oral formulations of the novel histone deacetylase inhibitor suberoylanilide hydroxamic acid in patients with advanced hematologic malignancies. *J.Clin.Oncol.* **24**: 166-73.

59. Mayo MW, Denlinger CE, Broad RM *et al.* (2003) Ineffectiveness of histone deacetylase inhibitors to induce apoptosis involves the transcriptional activation of NF-kappa B through the Akt pathway. *J.Biol.Chem.* **278**: 18980-9.

60. Catley L, Weisberg E, Kiziltepe T *et al.* (2006) Aggresome induction by proteasome inhibitor bortezomib and alpha-tubulin hyperacetylation by tubulin deacetylase (TDAC) inhibitor LBH589 are synergistic in myeloma cells. *Blood* **108**: 3441-9.

61. Dasmahapatra G, Rahmani M, Dent P, Grant S (2006) The tyrphostin adaphostin interacts synergistically with proteasome inhibitors to induce apoptosis in human leukemia cells through a reactive oxygen species (ROS)-dependent mechanism. *Blood* **107**: 232-40.

62. Ruefli AA, Ausserlechner MJ, Bernhard D *et al.* (2001) The histone deacetylase inhibitor and chemotherapeutic agent suberoylanilide hydroxamic acid (SAHA) induces a cell-death pathway characterized by cleavage of Bid and production of reactive oxygen species. *Proc.Natl.Acad.Sci.U.S.A* **98**: 10833-8.

63. Ling YH, Liebes L, Zou Y, Perez-Soler R (2003) Reactive oxygen species generation and mitochondrial dysfunction in the apoptotic response to Bortezomib, a novel proteasome inhibitor, in human H460 non-small cell lung cancer cells. *J.Biol.Chem.* **278**: 33714-23.

64. Johnson NA, Boyle M, Bashashati A *et al.* (2009) Diffuse large B-cell lymphoma: reduced CD20 expression is associated with an inferior survival. *Blood* **113**: 3773-80.

65. Goy A, Younes A, McLaughlin P *et al.* (2005) Phase II study of proteasome inhibitor bortezomib in relapsed or refractory B-cell non-Hodgkin's lymphoma. *J.Clin.Oncol.* **23**: 667-75.

66. Tournier C, Hess P, Yang DD *et al.* (2000) Requirement of JNK for stress-induced activation of the cytochrome c-mediated death pathway. *Science* **288**: 870-4.

67. Yang Y, Ikezoe T, Saito T, Kobayashi M, Koeffler HP, Taguchi H (2004) Proteasome inhibitor PS-341 induces growth arrest and apoptosis of non-small cell lung cancer cells via the JNK/c-Jun/AP-1 signaling. *Cancer Sci.* **95**: 176-80.

68. Li Y, Arita Y, Koo Hc, Davis JM, Kazzaz JA (2003) Inhibition of JNK Pathway Improves Cell Viability in Response to Oxidant Injury. *Am.J.Respir.Cell Mol.Biol.* 2003-0087RC.

VITA

Dmitry Lembersky was born April 20, 1985 in Zaporozhye, Ukraine, and moved to the United States in 1994 at the age of 9. He received his Bachelor of Science degree in Biology and a minor in Chemistry from Christopher Newport University, Newport News, VA in May of 2007, and received his Master of Science in Biochemistry from Virginia Commonwealth University, Richmond, VA in May of 2009.